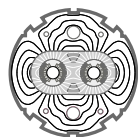


EUROPEAN ORGANIZATION FOR NUCLEAR RESEARCH  
European Laboratory for Particle Physics



*Large Hadron Collider Project*

**LHC Project Report 369**

**6D Beam-Beam Kick including Coupled Motion**

L.H.A. Leunissen, G. Ripken, F. Schmidt, CERN, SL-Division, Geneva, Switzerland

**Abstract**

The 6D beam-beam interaction as developed in 1992 by Hirata, Moshhammer and Ruggiero [1,2] has been extended to include linear coupled motion and an arbitrary crossing plane. The technique of symplectic mapping in the six-dimensional phase space, called synchro-beam mapping (SBM), is applied to investigate the beam-beam kick within a solenoid. A linear beam-beam model including coupling is discussed in detail, also in the framework of a six-dimensional symplectic dispersion formalism.

Administrative Secretariat  
LHC Division  
CERN  
CH-1211 Geneva 23  
Switzerland

Geneva, 4 February 2000

## Contents

1	<b>Introduction</b>	<b>1</b>
2	<b>Beam-beam kick for coupled motion</b>	<b>1</b>
2.1	<i>The electromagnetic field due to a tilted bunch</i>	<i>1</i>
2.1.1	Test particle	2
2.1.2	Strong bunch	2
2.2	<i>Lorentz boost</i>	<i>3</i>
2.2.1	Transformation from Cartesian to accelerator coordinates	4
2.2.2	Arbitrary crossing plane	5
2.2.3	Full Lorentz boost	6
2.3	<i>Beam-beam force</i>	<i>8</i>
3	<b>Summary</b>	<b>14</b>
	Appendix A: Calculation of the coupling angle in the $X - Y$ plane	15
A1:	Coupling angle in the physical $X - Y$ plane	17
	Appendix B: Synchro Beam Mapping within Solenoid Fields	19
	Appendix C: Linear Beam-Beam model	28
	Appendix D: Dispersion formalism including the beam-beam kick	30
D1:	Canonical Transformation	30
D2:	The Eigenvalue Spectrum of the Orbital Revolution Matrix	36
D3:	Decoupled Motion; Twiss Parameters	37
	List of symbols	39
	Acknowledgements	41
	Bibliography	41

## 1 Introduction

The beam-beam interaction is studied in storage rings, using the formalism developed by Hirata, Moshhammer and Ruggiero (synchro-beam mapping and a Lorentz boost transforming the collision with a crossing angle to a head-on collision). In this approach the strong bunch is split longitudinally into several slices, where each slice is described by an electrostatic potential of the form

$$U(x, y; \Sigma_{11}, \Sigma_{33}) = -\frac{r_p}{\gamma_0} \int_0^\infty \frac{\exp\left(-\frac{x^2}{2\Sigma_{11} + u} - \frac{y^2}{2\Sigma_{33} + u}\right)}{\sqrt{2\Sigma_{11} + u} \sqrt{2\Sigma_{33} + u}} du. \quad (1.1)$$

Here  $r_p$  is the classical particle radius,  $\gamma_0$  is the Lorentz factor of the test particle and  $\underline{\Sigma}$  is the  $6 \times 6$  phase-space envelope matrix of the strong bunch defined by

$$\Sigma_{ij} \equiv \langle X_i X_j \rangle - \langle X_i \rangle \langle X_j \rangle, \quad i, j = 1, \dots, 6 \quad (1.2)$$

where the lowercase  $x, y$  and the uppercase  $X, Y$  stand for the transverse coordinates of the test particle and the strong bunch with  $\vec{X} = (X, P_X; Y, P_Y; Z, P_Z)^T$ , respectively. In addition, a new technique of symplectic mapping in the six-dimensional phase space, called synchro-beam mapping (SBM), has been introduced by these authors in Ref. [1]. It allows to include the bunch length effect at the collision point and the energy variation caused by the electric field of the opposite bunch. This mapping is formulated only for head-on collision, but Hirata has shown that a crossing angle can be eliminated by a Lorentz-boost [2].

Eq. (1.1) is valid for the case of uncoupled motion. The aim of this report is to extend the formalism so as to include six-dimensional linear coupling.

This paper is organised as follows: In section 2 the beam-beam kick is studied in the most general form. The tilted cross section induced by coupling, which is needed in section 2 is calculated in appendix A. In Appendix B we describe methods to construct SBM-solutions for a solenoid field which allow us to investigate the beam-beam kick within a solenoid. The SBM-solution is obtained by the use of a generating function, of Lie-series or by an integration method. A linear model of the beam-beam kick including coupling is studied in Appendices C and D, concerning the derivation of the linear beam-beam matrix, the tune-shift caused by a beam-beam kick and a linear six-dimensional dispersion formalism including the beam-beam interaction. Lastly, a summary of the results is presented in section 3. The 6D beam-beam formalism has been incorporated in the tracking programs MAD [3] and SixTrack [4].

## 2 Beam-beam kick for coupled motion

### 2.1 The electromagnetic field due to a tilted bunch

The generalisation of the analysis in Refs. [1, 2] by including coupling and a tilted strong bunch (caused by coupling) can be achieved in a straightforward manner by describing the particle motion in the framework of the fully coupled six-dimensional formalism and by replacing the electric potential  $U$  of Eq. (1.1) for an untilted bunch by a new potential

$$\hat{U}(x, y; \hat{\Sigma}_{11}, \hat{\Sigma}_{33}; \theta) \equiv U(\hat{x}, \hat{y}; \hat{\Sigma}_{11}, \hat{\Sigma}_{33}) = -\frac{r_p}{\gamma_0} \int_0^\infty \frac{\exp\left(-\frac{\hat{x}^2}{2\hat{\Sigma}_{11} + u} - \frac{\hat{y}^2}{2\hat{\Sigma}_{33} + u}\right)}{\sqrt{2\hat{\Sigma}_{11} + u} \sqrt{2\hat{\Sigma}_{33} + u}} du, \quad (2.3)$$

where the symbol ‘ $\hat{\cdot}$ ’ denotes quantities in the coupled frame of reference. The coupling has to be considered for the test particle as well as for the strong bunch.

### 2.1.1 Test particle

The potential (2.3) is obtained from (1.1) by introducing a rotated coordinate system of the test particle (for details see Appendix A):

$$\begin{aligned}\hat{x} &= x \cos \theta + y \sin \theta; \\ \hat{y} &= -x \sin \theta + y \cos \theta\end{aligned}\tag{2.4}$$

where  $\theta$  denotes the coupling angle of the strong bunch given by <sup>1)</sup>:

$$\begin{aligned}\sin 2\theta &= -\text{sgn}(\Sigma_{11} - \Sigma_{33}) \cdot \frac{2\Sigma_{13}}{\sqrt{[\Sigma_{11} - \Sigma_{33}]^2 + 4\Sigma_{13}^2}}; \\ \cos 2\theta &= \text{sgn}(\Sigma_{11} - \Sigma_{33}) \cdot \frac{(\Sigma_{11} - \Sigma_{33})}{\sqrt{[\Sigma_{11} - \Sigma_{33}]^2 + 4\Sigma_{13}^2}}; \\ \implies \tan 2\theta &= -\frac{2\Sigma_{13}}{\Sigma_{11} - \Sigma_{33}}\end{aligned}\tag{2.5}$$

or

$$\begin{aligned}\sin \theta &= -\text{sgn}\{(\Sigma_{11} - \Sigma_{33})\Sigma_{13}\} \sqrt{\frac{1}{2}(1 - \cos 2\theta)} \\ \cos \theta &= \sqrt{\frac{1}{2}(1 + \cos 2\theta)}.\end{aligned}\tag{2.6}$$

### 2.1.2 Strong bunch

For the strong beam we have the same transformation (2.4) for  $X$  and  $Y$  among the coordinates  $\vec{X} \equiv (X, P_X; Y, P_Y; Z, P_Z)^T$ . The linear particle motion can be represented as a superposition of eigenmodes as shown in [5]. Denoting by  $J_k$  and  $\phi_k$  ( $k = I, II, III$ ) the action-angle variables

$$\vec{X}(s) = \sum_{k=I,II,III} \sqrt{J_k} [\vec{v}_k(s) e^{-i\phi_k} + \vec{v}_k^* e^{i\phi_k}]\tag{2.7}$$

where  $\vec{v}_k(s)$  ( $k = I, II, III$ ) describe the eigenmotion with the linear 6D transfer matrix from longitudinal position  $s_0$  to  $s$ :

$$\vec{v}_k(s) = M(s, s_0) \vec{v}_k(s_0)\tag{2.8}$$

with

$$M(s_0 + L, s_0) \vec{v}_k(s_0) = e^{-i2\pi Q_k} \vec{v}_k(s_0)\tag{2.9}$$

---

<sup>1)</sup> We have chosen  $\theta = -\theta_p$  defined in Appendix A, since the strong bunch rotates in the opposite direction of the test particle. In a double-ring machine such as the LHC this is not necessarily true.

( $L$  is the circumference of the accelerator and  $Q_k$  the tune for the  $k^{\text{th}}$  mode). The rotated  $\hat{\Sigma}$  can be expressed by the elements of the unrotated  $\Sigma$ -matrix:

$$\begin{aligned}\hat{\Sigma}_{11} \equiv \langle \hat{X}^2 \rangle &= \frac{1}{2} \left\{ [\Sigma_{11} + \Sigma_{33}] + \text{sgn}(\Sigma_{11} - \Sigma_{33}) \sqrt{[\Sigma_{11} - \Sigma_{33}]^2 + 4\Sigma_{13}^2} \right\} \\ \hat{\Sigma}_{33} \equiv \langle \hat{Y}^2 \rangle &= \frac{1}{2} \left\{ [\Sigma_{11} + \Sigma_{33}] - \text{sgn}(\Sigma_{11} - \Sigma_{33}) \sqrt{[\Sigma_{11} - \Sigma_{33}]^2 + 4\Sigma_{13}^2} \right\}.\end{aligned}\tag{2.10}$$

These elements are a function of the eigenvectors:

$$\begin{aligned}\Sigma_{11} \equiv \langle X^2 \rangle &= \sum_{k=I,II,III} 2J_k v_{k1} v_{k1}^*; \\ \Sigma_{33} \equiv \langle Y^2 \rangle &= \sum_{k=I,II,III} 2J_k v_{k3} v_{k3}^*; \\ \Sigma_{13} \equiv \langle XY \rangle &= \sum_{k=I,II,III} J_k [v_{k1} v_{k3}^* + v_{k1}^* v_{k3}].\end{aligned}\tag{2.11}$$

Note that

$$E_1 = \sqrt{\hat{\Sigma}_{11}}, \quad E_2 = \sqrt{\hat{\Sigma}_{33}}\tag{2.12}$$

are the principal axes of the elliptical cross section

$$\frac{\hat{X}^2}{E_1} + \frac{\hat{Y}^2}{E_2} = 1\tag{2.13}$$

in the  $(\hat{X} - \hat{Y})$ -plane.

Conversely to Ref. [2], the crossing angle  $2\phi$  can be chosen in an arbitrary crossing plane  $(\tilde{x} - s)$ , defined by an angle  $\alpha$  (see Fig. 1). We can write the components of the strong bunch in a Cartesian coordinate system  $(X, Y, Z; P_x, P_y, P_z)$  defined for the laboratory frame and oriented according to the ideal orbit of the test particle as:

$$\begin{aligned}P_x &= P \sin 2\phi \cos \alpha; \\ P_y &= P \sin 2\phi \sin \alpha; \\ P_z &= -P \cos 2\phi,\end{aligned}\tag{2.14}$$

with  $P$  the momentum of the bunch.

## 2.2 Lorentz boost

The Lorentz boost as described by Hirata consists of a transformation of Cartesian to accelerator coordinates and a Lorentz boost which makes the collision between the bunches head-on. This is necessary because the 6D beam-beam interaction is only described for a head-on collision. In addition, we include the crossing plane angle  $\alpha$  in our formalism.

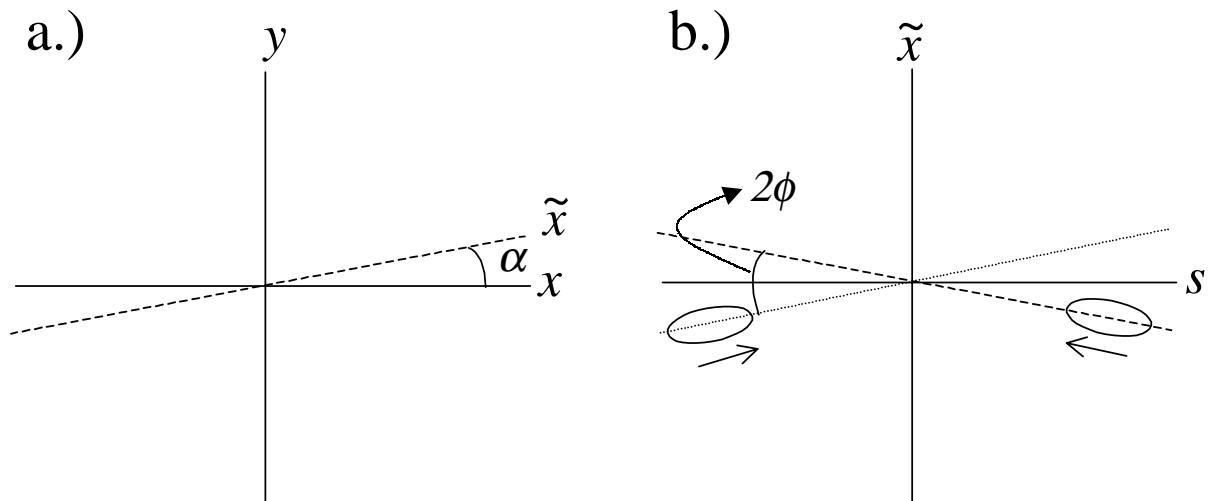


Figure 1: Part a.) defines the crossing plane angle  $\alpha$  in the  $(x - y)$ -plane and part b.) depicts the total crossing angle  $2\phi$  in the  $(\tilde{x} - s)$ -plane.

### 2.2.1 Transformation from Cartesian to accelerator coordinates

The following relations of Ref. [2] remain valid:

$$\begin{pmatrix} ct \\ x_C \\ z_C \\ y_C \end{pmatrix} = \underline{A} \begin{pmatrix} z(s) \\ x(s) \\ s \\ y(s) \end{pmatrix}, \quad (2.15)$$

where

$$\underline{A} = \underline{A}^{-1} = \begin{pmatrix} -1 & 0 & 1 & 0 \\ 0 & 1 & 0 & 0 \\ 0 & 0 & 1 & 0 \\ 0 & 0 & 0 & 1 \end{pmatrix} \quad (2.16)$$

and

$$\begin{pmatrix} E/c - p_0 \\ p_{xC} \\ p_{zC} - p_0 \\ p_{yC} \end{pmatrix} = p_0 \underline{B} \begin{pmatrix} p_z \\ p_x \\ h \\ p_y \end{pmatrix}, \quad (2.17)$$

with

$$\underline{B} = \underline{B}^{-1} = \begin{pmatrix} 1 & 0 & 0 & 0 \\ 0 & 1 & 0 & 0 \\ 1 & 0 & -1 & 0 \\ 0 & 0 & 0 & 1 \end{pmatrix} \quad (2.18)$$

and  $p_0$  being the momentum of the test particle. They describe the connection between the Cartesian coordinate  $(x_C, p_{xC}; y_C, p_{yC}; z_C, p_{zC}; E, t)$  with  $E = cp$  and the accelerator coordinate  $\vec{x} = (x, p_x; y, p_y; z, p_z; h, s)$  of the test particle with the Hamiltonian

$$h(p_x, p_y, p_z) = p_z + 1 - \sqrt{(p_z + 1)^2 - p_x^2 - p_y^2}. \quad (2.19)$$

In this case we applied the ultrarelativistic approximation  $v_0 \approx c$ .

The Lorentz transformation

$$\underline{L}_0 = \begin{pmatrix} 1/\cos\phi & -\sin\phi & -\tan\phi\sin\phi & 0 \\ -\tan\phi & 1 & \tan\phi & 0 \\ 0 & -\sin\phi & \cos\phi & 0 \\ 0 & 0 & 0 & 1 \end{pmatrix} \quad (2.20)$$

used in Ref. [2] makes the collision as if head-on for  $\alpha = 0$  so that the synchro-beam mapping can be applied.

### 2.2.2 Arbitrary crossing plane

We now include the crossing plane angle  $\alpha$  by the following similarity transformation:

$$\underline{L} = \underline{R}^{-1} \underline{L}_0 \underline{R} \quad (2.21)$$

with

$$\underline{R} = \begin{pmatrix} 1 & 0 & 0 & 0 \\ 0 & \cos\alpha & 0 & \sin\alpha \\ 0 & 0 & 1 & 0 \\ 0 & -\sin\alpha & 0 & \cos\alpha \end{pmatrix} \quad (2.22)$$

or

$$\underline{L} = \begin{pmatrix} 1/\cos\phi & -\cos\alpha\sin\phi & -\tan\phi\sin\phi & -\sin\alpha\sin\phi \\ -\cos\alpha\tan\phi & 1 & \cos\alpha\tan\phi & 0 \\ 0 & -\cos\alpha\sin\phi & \cos\phi & -\sin\alpha\sin\phi \\ -\sin\alpha\tan\phi & 0 & \sin\alpha\tan\phi & 1 \end{pmatrix}. \quad (2.23)$$

In order to interpret  $\underline{L}$  in Eq. (2.21) we may introduce a new coordinate system

$$\begin{pmatrix} \tilde{x} \\ \tilde{y} \end{pmatrix} = \begin{pmatrix} \cos\alpha & \sin\alpha \\ -\sin\alpha & \cos\alpha \end{pmatrix} \begin{pmatrix} x \\ y \end{pmatrix}, \quad (2.24)$$

corresponding to  $\underline{R}$ . Then the crossing plane is identical with the  $(\tilde{x} - s)$ -plane (see Figure 1). Since  $\underline{L}_0$  can be written in the form

$$\underline{L}_0 = \underbrace{\begin{pmatrix} 1/\cos\phi & -\tan\phi & 0 & 0 \\ -\tan\phi & 1/\cos\phi & 0 & 0 \\ 0 & 0 & 1 & 0 \\ 0 & 0 & 0 & 1 \end{pmatrix}}_{\text{Boost in the direction of the rotated } \tilde{x}\text{-axis}} \underbrace{\begin{pmatrix} 1 & 0 & 0 & 0 \\ 0 & \cos\phi & \sin\phi & 0 \\ 0 & -\sin\phi & \cos\phi & 0 \\ 0 & 0 & 0 & 1 \end{pmatrix}}_{\text{Rotation in the } (s - \tilde{x})\text{-plane}} \quad (2.25)$$

we define a second coordinate system

$$\begin{pmatrix} \bar{x} \\ \bar{s} \end{pmatrix} = \begin{pmatrix} \cos\phi & \sin\phi \\ -\sin\phi & \cos\phi \end{pmatrix} \begin{pmatrix} \tilde{x} \\ s \end{pmatrix}. \quad (2.26)$$

Then we are left with a boost in the direction of  $\bar{x}$  representing the rotated  $\tilde{x}$ -axis:

$$\begin{pmatrix} t^* \\ \bar{x}^* \end{pmatrix} = \begin{pmatrix} 1/\cos\phi & -\tan\phi \\ -\tan\phi & 1/\cos\phi \end{pmatrix} \begin{pmatrix} t \\ \bar{x} \end{pmatrix}. \quad (2.27)$$

### 2.2.3 Full Lorentz boost

As a result of the Lorentz boost we have:

$$\begin{pmatrix} cT^* \\ X^* \\ Z^* \\ Y^* \end{pmatrix} = \underline{L} \begin{pmatrix} cT \\ X \\ Z \\ Y \end{pmatrix}; \quad (2.28)$$

$$\begin{pmatrix} E^*/c \\ P_X^* \\ P_Z^* \\ P_Y^* \end{pmatrix} = \underline{L} \begin{pmatrix} E/c \\ P_X \\ P_Z \\ P_Y \end{pmatrix}. \quad (2.29)$$

Inserting Eq. (2.14) into Eq. (2.29), we get for the transformed momentum of the strong bunch ( $E/c = P$ ):  $P_x^* = 0$ ;  $P_y^* = 0$  since

$$\begin{aligned} P_x^* &= -P \cos \alpha \tan \phi + P \sin 2\phi \cos \alpha - P \cos \alpha \tan \phi \cos 2\phi \\ &= -P \cos \alpha \tan \phi \left[ 1 - \frac{\cos \phi}{\sin \phi} 2 \sin \phi \cos \phi + (\cos^2 \phi - \sin^2 \phi) \right] \\ &= -P \cos \alpha \tan \phi [1 - 2 \cos^2 \phi + \cos^2 \phi - \sin^2 \phi] \\ &= 0; \end{aligned} \quad (2.30)$$

$$\begin{aligned} P_y^* &= -P \sin \alpha \tan \phi - P \sin \alpha \tan \phi \cos 2\phi + P \sin 2\phi \sin \alpha \\ &= 0. \end{aligned}$$

For the test particle  $p_x = p_y = 0$ ,  $E = cp_0$  is transformed into  $p_x^* = p_y^* = 0$  and  $E^* = cp_0^* = cp_0 \cos \phi$ , i.e. the collision is indeed head-on.

Using Eq. (2.23), the full Lorentz transformation is therefore a transformation from the accelerator coordinates to Cartesian coordinates, the Lorentz transformation and again a backwards transformation to the accelerator coordinates:

$$\vec{x}(0) \rightarrow \vec{x}^*(s^*) \quad (2.31)$$

leading to:

$$\begin{pmatrix} z^*(s^*) \\ x^*(s^*) \\ s^* \\ y^*(s^*) \end{pmatrix} = \underline{A}^{-1} \underline{L} \underline{A} \begin{pmatrix} z(0) \\ x(0) \\ 0 \\ y(0) \end{pmatrix} = \begin{pmatrix} 1/\cos \phi & 0 & 0 & 0 \\ \cos \alpha \tan \phi & 1 & 0 & 0 \\ 0 & -\cos \alpha \sin \phi & \cos \phi & -\sin \alpha \sin \phi \\ \sin \alpha \tan \phi & 0 & 0 & 1 \end{pmatrix} \begin{pmatrix} z(0) \\ x(0) \\ 0 \\ y(0) \end{pmatrix} \quad (2.32)$$



and

$$\begin{pmatrix} p_z^*(s^*) \\ p_x^*(s^*) \\ h^* \\ p_y^*(s^*) \end{pmatrix} = \frac{p_0}{p_0^*} \underline{B}^{-1} \underline{L} \underline{B} \begin{pmatrix} p_z(0) \\ p_x(0) \\ h \\ p_y(0) \end{pmatrix} = \begin{pmatrix} 1 & -\cos \alpha \tan \phi & \tan^2 \phi & -\sin \alpha \tan \phi \\ 0 & 1/\cos \phi & -\cos \alpha \frac{\tan \phi}{\cos \phi} & 0 \\ 0 & 0 & 1/\cos^2 \phi & 0 \\ 0 & 0 & -\sin \alpha \frac{\tan \phi}{\cos \phi} & 1/\cos \phi \end{pmatrix} \begin{pmatrix} p_z(0) \\ p_x(0) \\ h \\ p_y(0) \end{pmatrix}. \quad (2.33)$$

From Eq. (2.32) we have:

$$s^* = -x(0) \cos \alpha \sin \phi - y(0) \sin \alpha \sin \phi \quad (2.34)$$

so that in general  $s = 0$  is not necessarily transformed to  $s^* = 0$ . Since we need a transformation from  $\vec{x}(0)$  to  $\vec{x}^*(0^*)$ , an additional transformation

$$\vec{x}^*(s^*) \rightarrow \vec{x}^*(0^*) \quad (2.35)$$

has to be performed.

Following Ref. [2], the transformation (2.35) can be written as a first-order Taylor expansion:

$$\begin{aligned} w_i^*(0^*) &= w_i^*(s^*) - \frac{dw_i^*(0^*)}{ds^*} s^* \\ &= w_i^*(s^*) - h_i^* s^* \\ &= w_i^*(s^*) + h_i^* \sin \phi [x(0) \cos \alpha + y(0) \sin \alpha] \end{aligned} \quad (2.36)$$

with

$$w_i \equiv (x, y, z); \quad h_i^* = \frac{\partial}{\partial p_i^*} h^*(p_x^*, p_y^*, p_z^*; p_0^*). \quad (2.37)$$

Furthermore we obtain from (2.33) and the Hamiltonian (2.19):

$$h^*(p_x^*, p_y^*, p_z^*; p_0^*) = \frac{1}{\cos^2 \phi} h(p_x, p_y, p_z; p_0) = h(p_x^*, p_y^*, p_z^*; p_0^*). \quad (2.38)$$

Combining the transformations (2.32, 2.33) and (2.36), we finally obtain the equations:

$$\begin{aligned}
x^* &= z \cos \alpha \tan \phi + x + h_x^* [x \cos \alpha \sin \phi + y \sin \alpha \sin \phi] \\
&= z \cos \alpha \tan \phi + x [1 + h_x^* \cos \alpha \sin \phi] + y h_x^* \sin \alpha \sin \phi; \\
y^* &= z \sin \alpha \tan \phi + y + h_y^* [x \cos \alpha \sin \phi + y \sin \alpha \sin \phi] \\
&= z \sin \alpha \tan \phi + y [1 + h_y^* \sin \alpha \sin \phi] + x h_y^* \cos \alpha \sin \phi; \\
z^* &= \frac{z}{\cos \phi} + h_z^* [x \cos \alpha \sin \phi + y \sin \alpha \sin \phi];
\end{aligned} \tag{2.39}$$

$$p_x^* = \frac{p_x}{\cos \phi} - h \cos \alpha \frac{\tan \phi}{\cos \phi};$$

$$p_y^* = \frac{p_y}{\cos \phi} - h \sin \alpha \frac{\tan \phi}{\cos \phi};$$

$$p_z^* = p_z - p_x \cos \alpha \tan \phi - p_y \sin \alpha \tan \phi + h \tan^2 \phi$$

representing the result of a Lorentz boost applied to the coordinates of the test particle which makes the collision as if head-on.

The transformation  $\mathcal{L}$  of Eq. (2.39) can be represented as the combination of a scale transformation

$$(x, y, z; p_x, p_y, p_z) \rightarrow (\tilde{x}, \tilde{y}, \tilde{z}; \tilde{p}_x, \tilde{p}_y, \tilde{p}_z) \tag{2.40}$$

with

$$\tilde{x} = x, \quad \tilde{y} = y, \quad \tilde{z} = z;$$

$$\tilde{p}_x = \frac{p_x}{\cos \phi}, \quad \tilde{p}_y = \frac{p_y}{\cos \phi}, \quad \tilde{p}_z = \frac{p_z}{\cos \phi} \tag{2.41}$$

and a canonical transformation

$$(\tilde{x}, \tilde{y}, \tilde{z}; \tilde{p}_x, \tilde{p}_y, \tilde{p}_z) \rightarrow (x^*, y^*, z^*; p_x^*, p_y^*, p_z^*) \tag{2.42}$$

resulting from the generating function

$$F_2(\tilde{x}, \tilde{y}, \tilde{z}; p_x^*, p_y^*, p_z^*) = \tilde{x} p_x^* + \tilde{y} p_y^* + \frac{\tilde{z}}{\cos \phi} p_z^* + \tag{2.43}$$

$$\tilde{z} \tan \phi [p_x^* \cos \alpha + p_y^* \sin \alpha] + \sin \phi [\tilde{x} \cos \alpha + \tilde{y} \sin \alpha] h^* (p_x^*, p_y^*, p_z^*).$$

Thus  $\mathcal{L}$  is only quasi-symplectic; the Jacobian of this transformation is  $1/\cos^3 \phi$ . This lack of symplecticity is restored in the backwards transformation  $\mathcal{L}^{-1}$  after having applied the beam-beam force.

### 2.3 Beam-beam force

We approximate the strong bunch by a number of slices. Each slice is represented by its  $Z^*(0^*)$  coordinate, which shall be denoted by  $Z^\dagger$ . Taking into account only terms linear

with respect to dynamical variables in  $\mathcal{L}$ , the first and second momenta of the particle distribution at the locations of the slices are given by:

$$\begin{aligned}
X^\dagger &= Z^\dagger \cos \alpha \sin \phi; & P_X^\dagger &= 0; \\
Y^\dagger &= Z^\dagger \sin \alpha \sin \phi; & P_Y^\dagger &= 0; \\
P_Z^\dagger &= 0; \\
\Sigma_{11}^\dagger &= \Sigma_{11}; & \Sigma_{22}^\dagger &= \frac{1}{\cos^2 \phi} \Sigma_{22}; \\
\Sigma_{33}^\dagger &= \Sigma_{33}; & \Sigma_{44}^\dagger &= \frac{1}{\cos^2 \phi} \Sigma_{44}; \\
\Sigma_{12}^\dagger &= \frac{1}{\cos \phi} \Sigma_{12}; & \Sigma_{13}^\dagger &= \Sigma_{13}; \\
\Sigma_{14}^\dagger &= \frac{1}{\cos \phi} \Sigma_{14}; & \Sigma_{23}^\dagger &= \frac{1}{\cos \phi} \Sigma_{23}; \\
\Sigma_{24}^\dagger &= \frac{1}{\cos^2 \phi} \Sigma_{24}; & \Sigma_{34}^\dagger &= \frac{1}{\cos \phi} \Sigma_{34}.
\end{aligned} \tag{2.44}$$

Inserting Eq. (2.44) into Eqs. (2.5) and (2.10) one obtains:

$$\begin{aligned}
\theta^\dagger &= \theta; \\
\hat{\Sigma}_{11}^\dagger &= \hat{\Sigma}_{11}; & \hat{\Sigma}_{33}^\dagger &= \hat{\Sigma}_{33}; & \hat{\Sigma}_{13}^\dagger &= \hat{\Sigma}_{13},
\end{aligned} \tag{2.45}$$

i.e. the cross section of the strong bunch remains unchanged.

In order to calculate the beam-beam kick, we need to transform  $\hat{\Sigma}_{11}^\dagger$  and  $\hat{\Sigma}_{33}^\dagger$  as well as  $\theta^\dagger$  from the interaction point (IP) to the collision point (CP). The distance between the two points is given by

$$S = S(z^*, Z^\dagger) = \frac{z^* - Z^\dagger}{2} \tag{2.46}$$

Using Eqs. (2.5), (2.10) and (2.44) we obtain:

$$\begin{aligned}
\hat{\Sigma}_{11}^\dagger(S) &= \frac{1}{2} \left\{ [\Sigma_{11}^\dagger(S) + \Sigma_{33}^\dagger(S)] \right. \\
&\quad \left. + \text{sgn}(\Sigma_{11}^\dagger(S) - \Sigma_{33}^\dagger(S)) \sqrt{[\Sigma_{11}^\dagger(S) - \Sigma_{33}^\dagger(S)]^2 + 4\Sigma_{13}^\dagger(S)^2} \right\}; \\
\hat{\Sigma}_{33}^\dagger(S) &= \frac{1}{2} \left\{ [\Sigma_{11}^\dagger(S) + \Sigma_{33}^\dagger(S)] \right. \\
&\quad \left. - \text{sgn}(\Sigma_{11}^\dagger(S) - \Sigma_{33}^\dagger(S)) \sqrt{[\Sigma_{11}^\dagger(S) - \Sigma_{33}^\dagger(S)]^2 + 4\Sigma_{13}^\dagger(S)^2} \right\},
\end{aligned} \tag{2.47}$$

i.e. we obtain the same result for a slice and the whole bunch, respectively. In a drift space (e.g. the horizontal plane),

$$X(S) = X(0) + P_X(0)S; \quad P_X(S) = P_X(0) \tag{2.48}$$

we have

$$\begin{aligned}
\Sigma_{11}^\dagger(S) &= \Sigma_{11}^\dagger(0) + 2\Sigma_{12}^\dagger(0)S + \Sigma_{22}^\dagger(0)S^2 \\
&= \Sigma_{11}(0) + 2\Sigma_{12}(0)\varphi + \Sigma_{22}(0)\varphi^2 \\
&\equiv \Sigma_{11}(\varphi); \\
\Sigma_{33}^\dagger(S) &= \Sigma_{33}^\dagger(0) + 2\Sigma_{34}^\dagger(0)S + \Sigma_{44}^\dagger(0)S^2 \\
&= \Sigma_{33}(0) + 2\Sigma_{34}(0)\varphi + \Sigma_{44}(0)\varphi^2 \\
&\equiv \Sigma_{33}(\varphi); \\
\Sigma_{13}^\dagger(S) &= \Sigma_{13}^\dagger(0) + [\Sigma_{14}^\dagger(0) + \Sigma_{23}^\dagger(0)]S + \Sigma_{24}^\dagger(0)S^2 \\
&= \Sigma_{13}(0) + [\Sigma_{14}(0) + \Sigma_{23}(0)]\varphi + \Sigma_{24}(0)\varphi^2 \\
&\equiv \Sigma_{13}(\varphi)
\end{aligned} \tag{2.49}$$

where  $\varphi = \frac{S}{\cos\phi}$ . Thus:

$$\begin{aligned}
\hat{\Sigma}_{11}^\dagger(S) &= \hat{\Sigma}_{11}(\varphi); \\
\hat{\Sigma}_{33}^\dagger(S) &= \hat{\Sigma}_{33}(\varphi); \\
\theta^\dagger(S) &= \theta(\varphi)
\end{aligned} \tag{2.50}$$

with  $\hat{\Sigma}_{11}$ ,  $\hat{\Sigma}_{33}$  and  $\theta$  given by (2.5) and (2.10).

The real collision between the test particle and the slice takes place at  $S$ , see Eq. (2.46). To calculate the beam-beam interaction, three subsequent transformations have to be performed. First, the test particle at the IP is brought to the CP by a drift. Then the beam-beam interaction is applied and finally the position of the test particle is brought back to the IP. This set of transformations is called the synchro-beam mapping (SBM) <sup>2)</sup>

It is convenient to introduce a new set of canonical variables at the collision point:

$$\begin{aligned}
\bar{x}^* &= x^* + Sp_x^* - X^\dagger(Z^\dagger); \\
\bar{y}^* &= y^* + Sp_y^* - Y^\dagger(Z^\dagger); \\
\bar{z}^* &= z^*
\end{aligned} \tag{2.51}$$

---

<sup>2)</sup> The SBM as described in detail in Ref. [1] can be represented by a Hamiltonian  $\mathcal{H} = \mathcal{H}_{bb}(\vec{x}^*)\delta(s^*)$  with  $\mathcal{H}_{bb}$  defined implicitly by

$$\exp(:\mathcal{H}_{bb}:) = \prod_{Z^\dagger} \exp(:n^*U(\hat{x}^*, \hat{y}^*; \hat{\Sigma}_{11}, \hat{\Sigma}_{33}):)$$

describing the interaction of a test particle in the weak bunch with a slice of the strong bunch represented by  $Z^\dagger$ .

and

$$\begin{aligned}
\bar{p}_x^* &= p_x^*; \\
\bar{p}_y^* &= p_y^*; \\
\bar{p}_z^* &= p_z^* - \frac{(p_x^*)^2 + (p_y^*)^2}{4}.
\end{aligned} \tag{2.52}$$

Here we have assumed a drift space between the IP and the CP. In these new variables, the SBM transformation can be written as concatenation of three symplectic transformations:

$$\exp(- : D :) \exp(: \mathcal{H}_{bb} :) \exp(: D :) \tag{2.53}$$

where

$$D(S) = \frac{(p_x^*)^2 + (p_y^*)^2}{2} S \tag{2.54}$$

In appendix B,  $D(S)$  is calculated in the presence of a solenoid field.

The particle-slice interaction at the CP finally leads to:

$$(\bar{x}^*, \bar{y}^*, \bar{z}^*) \rightarrow (\bar{x}^*, \bar{y}^*, \bar{z}^*) \tag{2.55}$$

and

$$\begin{aligned}
\bar{p}_x^* &\rightarrow \bar{p}_x^* - n^* F_x^*; \\
\bar{p}_y^* &\rightarrow \bar{p}_y^* - n^* F_y^*; \\
\bar{p}_z^* &\rightarrow \bar{p}_z^* - n^* F_z^*,
\end{aligned} \tag{2.56}$$

where  $n^*$  is the number of particles in the slice, i.e. the total number  $N^*$  divided by the number of slices, and

$$\begin{aligned}
F_x^* &= \frac{\partial}{\partial \bar{x}^*} \hat{U}(\bar{x}^*, \bar{y}^*; \hat{\Sigma}_{11}(\varphi), \hat{\Sigma}_{33}(\varphi); \theta(\varphi)); \\
F_y^* &= \frac{\partial}{\partial \bar{y}^*} \hat{U}(\bar{x}^*, \bar{y}^*; \hat{\Sigma}_{11}(\varphi), \hat{\Sigma}_{33}(\varphi); \theta(\varphi)); \\
F_z^* &= \frac{\partial}{\partial \bar{z}^*} \hat{U}(\bar{x}^*, \bar{y}^*; \hat{\Sigma}_{11}(\varphi), \hat{\Sigma}_{33}(\varphi); \theta(\varphi)) \\
&= \frac{1}{2} \frac{\partial}{\partial S} \hat{U}(\bar{x}^*, \bar{y}^*; \hat{\Sigma}_{11}(\varphi), \hat{\Sigma}_{33}(\varphi); \theta(\varphi))
\end{aligned} \tag{2.57}$$

with  $\hat{U}$  given by Eq. (2.3).

Introducing the variables

$$\begin{aligned}
\underline{x}^* &= w_1 \bar{x}^* + w_2 \bar{y}^*; \\
\underline{y}^* &= -w_2 \bar{x}^* + w_1 \bar{y}^*
\end{aligned} \tag{2.58}$$

(see Eq. (2.5)) with

$$w_1 = \cos \theta; \quad w_2 = \sin \theta, \quad (2.59)$$

we can also write:

$$\begin{aligned}
F_x^* &= \frac{\partial}{\partial \bar{x}^*} U(\underline{x}^*, \underline{y}^*; \hat{\Sigma}_{11}(\varphi), \hat{\Sigma}_{33}(\varphi)) \\
&= w_1(\varphi) \frac{\partial}{\partial \underline{x}^*} U(\underline{x}^*, \underline{y}^*; \hat{\Sigma}_{11}(\varphi), \hat{\Sigma}_{33}(\varphi)) \\
&\quad - w_2(\varphi) \frac{\partial}{\partial \underline{y}^*} U(\underline{x}^*, \underline{y}^*; \hat{\Sigma}_{11}(\varphi), \hat{\Sigma}_{33}(\varphi)); \\
F_y^* &= \frac{\partial}{\partial \bar{y}^*} U(\underline{x}^*, \underline{y}^*; \hat{\Sigma}_{11}(\varphi), \hat{\Sigma}_{33}(\varphi)) \\
&= w_2(\varphi) \frac{\partial}{\partial \underline{x}^*} U(\underline{x}^*, \underline{y}^*; \hat{\Sigma}_{11}(\varphi), \hat{\Sigma}_{33}(\varphi)) \\
&\quad + w_1(\varphi) \frac{\partial}{\partial \underline{y}^*} U(\underline{x}^*, \underline{y}^*; \hat{\Sigma}_{11}(\varphi), \hat{\Sigma}_{33}(\varphi)); \\
F_z^* &= \frac{1}{2} \frac{\partial}{\partial S} U(\underline{x}^*, \underline{y}^*; \hat{\Sigma}_{11}(\varphi), \hat{\Sigma}_{33}(\varphi)) \\
&= \frac{\partial U}{\partial \underline{x}^*} [w_1'(\varphi) \bar{x}^* + w_2'(\varphi) \bar{y}^*] \frac{1}{2 \cos \phi} \\
&\quad + \frac{\partial U}{\partial \underline{y}^*} [-w_2'(\varphi) \bar{x}^* + w_1'(\varphi) \bar{y}^*] \frac{1}{2 \cos \phi} \\
&\quad + \frac{\partial U}{\partial \hat{\Sigma}_{11}} \hat{\Sigma}'_{11}(\varphi) \frac{1}{2 \cos \phi} \\
&\quad + \frac{\partial U}{\partial \hat{\Sigma}_{33}} \hat{\Sigma}'_{33}(\varphi) \frac{1}{2 \cos \phi}
\end{aligned} \quad (2.60)$$

with  $U$  defined in Eq. (1.1) and the symbol “ $'$ ” indicating a differentiation with respect to  $\varphi$ .

Expressions for the terms  $\partial U / \partial \underline{x}^*$ ,  $\partial U / \partial \underline{y}^*$ ,  $\partial U / \partial \hat{\Sigma}_{11}$  and  $\partial U / \partial \hat{\Sigma}_{33}$  appearing in Eq. (2.60) can be found in Ref. [1] (see Eqs. (21), (22), (86), (87)) for a tri-gaussian distribution.

The terms  $\hat{\Sigma}'_{11}(\varphi)$  and  $\hat{\Sigma}'_{33}(\varphi)$  may be obtained by using Eqs. (2.10) and (2.11) and by taking into account, that the eigenvectors  $\vec{v}_k(s)$  ( $k = I, II, III$ ) obey the equations of

motion. For a drift space they read:

$$\begin{aligned}\frac{d}{ds}v_{k1} &= v_{k2}; \\ \frac{d}{ds}v_{k3} &= v_{k4}; \\ \frac{d}{ds}v_{k2} &= \frac{d}{ds}v_{k4} = 0.\end{aligned}\tag{2.61}$$

Alternatively, one can also use Eq. (2.10) in connection with Eq. (2.49). After some analysis one then obtains:

$$\begin{aligned}\hat{\Sigma}'_{11}(\varphi) &= 2 \left( \hat{\Sigma}_{12}(0) + \varphi \hat{\Sigma}_{22}(0) \right); \\ \hat{\Sigma}'_{33}(\varphi) &= 2 \left( \hat{\Sigma}_{34}(0) + \varphi \hat{\Sigma}_{44}(0) \right)\end{aligned}\tag{2.62}$$

with

$$\begin{aligned}\hat{\Sigma}_{12} &= \frac{1}{2} [(\Sigma_{12} + \Sigma_{34}) + \{(\Sigma_{12} - \Sigma_{34}) \cos 2\theta + (\Sigma_{14} + \Sigma_{23}) \sin 2\theta\}]; \\ \hat{\Sigma}_{34} &= \frac{1}{2} [(\Sigma_{12} + \Sigma_{34}) - \{(\Sigma_{12} - \Sigma_{34}) \cos 2\theta + (\Sigma_{14} + \Sigma_{23}) \sin 2\theta\}]; \\ \hat{\Sigma}_{22} &= \frac{1}{2} [(\Sigma_{22} + \Sigma_{44}) + \{(\Sigma_{22} - \Sigma_{44}) \cos 2\theta + 2\Sigma_{24} \sin 2\theta\}]; \\ \hat{\Sigma}_{44} &= \frac{1}{2} [(\Sigma_{22} + \Sigma_{44}) - \{(\Sigma_{22} - \Sigma_{44}) \cos 2\theta + 2\Sigma_{24} \sin 2\theta\}]\end{aligned}\tag{2.63}$$

where  $\sin 2\theta$  and  $\cos 2\theta$  are taken from Eq. (2.5).

The quantities  $w_1$  and  $w_2$  are determined by Eqs. (2.5) and (2.59). Lastly, in order to calculate  $w'_1(s)$  and  $w'_2(s)$  we use the relations

$$\begin{aligned}\cos 2\theta &= \cos^2 \theta - \sin^2 \theta \\ &= 2 \cos^2 \theta - 1 \\ &= 1 - 2 \sin^2 \theta\end{aligned}\tag{2.64}$$

$$\Rightarrow \begin{cases} w'_1(s) \equiv \frac{d}{ds} \cos \theta = \frac{1}{4 \cos \theta} \frac{d}{ds} \cos 2\theta; \\ w'_2(s) \equiv \frac{d}{ds} \sin \theta = -\frac{1}{4 \sin \theta} \frac{d}{ds} \cos 2\theta, \end{cases}$$

where  $\cos 2\theta$  has to be taken from Eq. (2.5).

Going back to the original coordinates, the explicit form for the complete SBM is

given by:

$$\begin{aligned}
x_{new}^* &= x^* + Sn^*F_x^* \\
p_{x,new}^* &= p_x^* - n^*F_x^* \\
y_{new}^* &= y^* + Sn^*F_y^* \\
p_{y,new}^* &= p_y^* - n^*F_y^* \\
z_{new}^* &= z^* \\
p_{z,new}^* &= p_z^* - \frac{1}{2} \left[ n^*F_x^*(p_x^* - \frac{1}{2}n^*F_x^*) + n^*F_y^*(p_y^* - \frac{1}{2}n^*F_y^*) \right] - n^*F_z^*
\end{aligned} \tag{2.65}$$

### 3 Summary

We have studied the beam-beam interaction for coupled motion in the framework of the weak-strong formalism taking into account a tilted cross section of the strong beam induced by linear coupling. This coupling has been included in the 6D beam-beam formalism of Hirata, Moshhammer and Ruggiero.

The extended formalism also allows for an arbitrary crossing plane. Furthermore, a SBM-solution for solenoid fields is derived which allows to investigate the beam-beam kick within a solenoid.

A linear model of the beam-beam kick, due to a tilted cross section of the strong bunch, is investigated in detail in Appendices C and D (beam-beam matrix and dispersion formalism including beam-beam interaction).

The equations derived in this report have been incorporated into the tracking codes MAD and SixTrack.



## Appendix A: Calculation of the coupling angle in the $X - Y$ plane

The aim of this appendix is to determine the angle  $\theta$  by which the principal axes of the beam ellipse are tilted in the physical  $(X - Y)$ -plane.

Linear particle motion can be written as a superposition of the three eigenvectors  $\vec{v}_k$  ( $k = I, II, III$ ):

$$\vec{X}(s) = \sum_{k=I,II,III} \sqrt{J_k} [\vec{v}_k(s) e^{-i\phi_k} + \vec{v}_k^*(s) e^{i\phi_k}] \quad (\text{A.1})$$

with  $\vec{X} \equiv (X, P_X, Y, P_Y, Z, P_Z)^T$ . For the eigenvectors holds:

$$\vec{v}_k(s) = M(s, s_0) \vec{v}_k(s_0) \quad (\text{A.2})$$

with

$$M(s_0 + L, s_0) \vec{v}_k(s_0) = e^{-i2\pi Q_k} \vec{v}_k(s_0) \quad (\text{A.3})$$

where  $L$  is the circumference of the accelerator and  $Q_k$  the tune for the  $k^{\text{th}}$  mode. They obey the orthogonality relations [5] ( $\vec{v}_k^+ \equiv (\vec{v}_k^T)^*$ ):

$$\begin{cases} \vec{v}_k^+(s_0) \underline{J} \vec{v}_k(s_0) = -\vec{v}_{-k}^+(s_0) \underline{J} \vec{v}_{-k}(s_0) = i; \\ \vec{v}_\mu^+(s_0) \underline{J} \vec{v}_\nu(s_0) = 0 \text{ otherwise,} \end{cases} \quad (\text{A.4})$$

with

$$\vec{v}_{-k} \equiv \vec{v}_k^* \quad (\text{A.5})$$

and

$$\underline{J} = \begin{pmatrix} 0 & -1 & 0 & 0 & 0 & 0 \\ 1 & 0 & 0 & 0 & 0 & 0 \\ 0 & 0 & 0 & -1 & 0 & 0 \\ 0 & 0 & 1 & 0 & 0 & 0 \\ 0 & 0 & 0 & 0 & 0 & -1 \\ 0 & 0 & 0 & 0 & 1 & 0 \end{pmatrix}. \quad (\text{A.6})$$

In particular one has:

$$X = \sum_{k=I,II,III} \sqrt{J_k} [v_{k1} e^{-i\phi_k} + v_{k1}^* e^{i\phi_k}]; \quad (\text{A.7})$$

$$Y = \sum_{k=I,II,III} \sqrt{J_k} [v_{k3} e^{-i\phi_k} + v_{k3}^* e^{i\phi_k}].$$

The rotation of the coordinates in the physical plane are given by:

$$\tilde{X} = X \cos \theta + Y \sin \theta; \quad (\text{A.8})$$

$$\tilde{Y} = -X \sin \theta + Y \cos \theta.$$

The rotated horizontal coordinate  $\tilde{X}$  reads:

$$\tilde{X}(\theta) = \sum_{k=I,II,III} \sqrt{J_k} [(v_{k1} \cos \theta + v_{k3} \sin \theta) e^{-i\phi_k} + (v_{k1}^* \cos \theta + v_{k3}^* \sin \theta) e^{i\phi_k}]. \quad (\text{A.9})$$

Averaging over the phase angles  $\phi_k$  we arrive at:

$$\frac{1}{2} \langle \tilde{X}^2(\theta) \rangle = \sum_{k=I,II,III} J_k [v_{k1} \cos \theta + v_{k3} \sin \theta] [v_{k1}^* \cos \theta + v_{k3}^* \sin \theta] \quad (\text{A.10})$$

leading to

$$E_h^2(\theta) = E_x^2 \cos^2 \theta + E_y^2 \sin^2 \theta + E_x G_x \sin 2\theta \quad (\text{A.11})$$

and using Eq. (2.11) we obtain

$$\begin{aligned} E_x^2 &= 2 \sum_{k=I,II,III} J_k v_{k1} v_{k1}^* \equiv \Sigma_{11}; \\ E_y^2 &= 2 \sum_{k=I,II,III} J_k v_{k3} v_{k3}^* \equiv \Sigma_{33}; \\ E_x G_x &= E_y G_y = \sum_{k=I,II,III} J_k [v_{k1} v_{k3}^* + v_{k1}^* v_{k3}] \equiv \Sigma_{13}; \\ E_h^2(\theta) &\equiv \langle \tilde{X}^2(\theta) \rangle. \end{aligned} \quad (\text{A.12})$$

For the vertical plane a similar solution can be obtained:

$$E_v^2(\theta) = E_x^2 \sin^2 \theta + E_y^2 \cos^2 \theta - E_y G_y \sin 2\theta = E_h^2(\theta + \pi/2) \quad (\text{A.13})$$

$E_h(\theta), E_v(\theta)$  are the maxima of the least squared amplitudes of the particle motion in  $\theta$ -direction.

The principal axes  $E_1, E_2$  can be found by maximising  $E_h^2(\theta) - E_v^2(\theta)$ . This yields  $\theta_p$

$$\tan 2\theta_p = \frac{2E_x G_x}{E_x^2 - E_y^2}. \quad (\text{A.14})$$

Choosing

$$\begin{aligned} \sin 2\theta_p &= \frac{2E_x G_x}{\mathcal{N}}; \\ \cos 2\theta_p &= \frac{E_x^2 - E_y^2}{\mathcal{N}} \end{aligned} \quad (\text{A.15})$$

we obtain

$$\begin{aligned} E_h^2(\theta_p) &= E_1^2 = \frac{1}{2} \{ [E_x^2 + E_y^2] + \mathcal{N} \} \equiv \langle \hat{X}^2 \rangle \\ E_v^2(\theta_p) &= E_2^2 = \frac{1}{2} \{ [E_x^2 + E_y^2] - \mathcal{N} \} \equiv \langle \hat{Y}^2 \rangle, \end{aligned} \quad (\text{A.16})$$

where  $\mathcal{N} = \pm \sqrt{[E_x^2 - E_y^2]^2 + 4(E_x G_x)^2}$ . The sign of  $\mathcal{N}$  may be chosen in such a way that  $\cos 2\theta_p$  becomes positive:

$$\mathcal{N} = \text{sgn}(E_x^2 - E_y^2) \sqrt{[E_x^2 - E_y^2]^2 + 4(E_x G_x)^2}, \quad (\text{A.17})$$

i.e.  $-\pi/4 \leq \theta_p \leq \pi/4$ . The beam ellipse with respect to the principal axes  $(\hat{X}, \hat{Y})$  can be written as

$$\frac{\hat{X}^2}{E_1^2} + \frac{\hat{Y}^2}{E_2^2} = 1. \quad (\text{A.18})$$

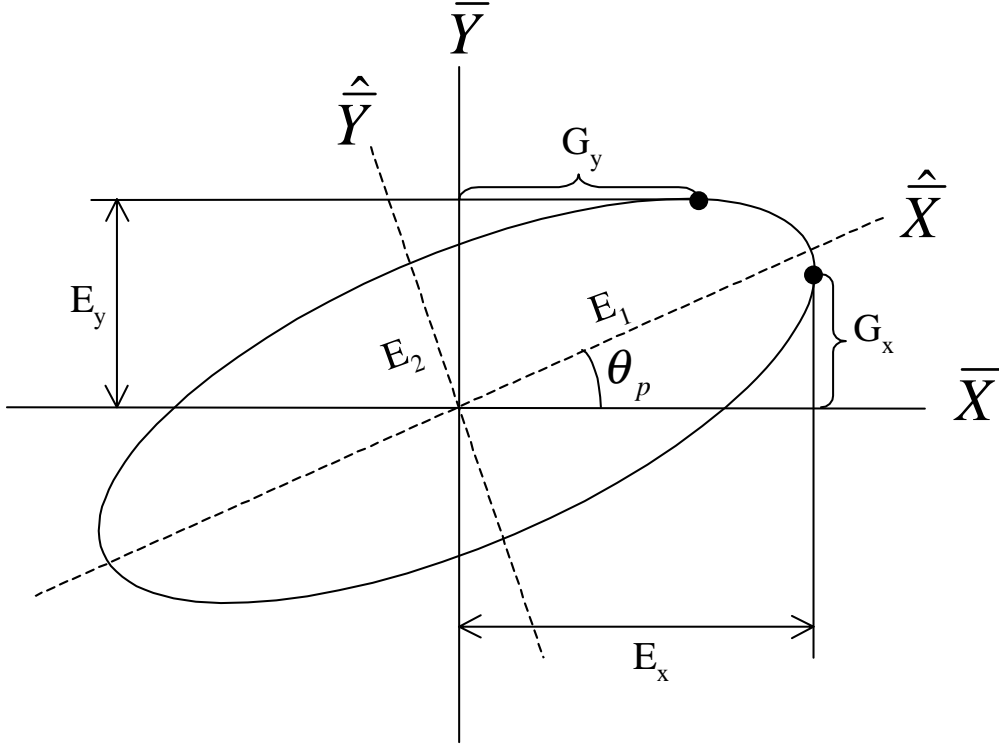


Figure 2: Cross section of the averaged plane ( $\bar{X} - \bar{Y}$ ).

Figure 2 illustrates the relation between  $E_x, E_y, G_x, G_y, E_1, E_2$  and  $\theta_p$ . Equation (A.18) can be rewritten for the averaged coordinates  $\bar{X}$  and  $\bar{Y}$

$$E_y^2 \bar{X}^2 - 2E_x G_x \bar{X} \bar{Y} + E_x^2 \bar{Y}^2 = E_1^2 E_2^2 = \epsilon^2, \quad (\text{A.19})$$

with

$$\epsilon^2 = E_x^2 (E_y^2 - G_x^2) = E_y^2 (E_x^2 - G_y^2) \quad (\text{A.20})$$

which has the following solution using an arbitrary angle  $\psi$ :

$$\begin{pmatrix} \bar{X}(\psi) \\ \bar{Y}(\psi) \end{pmatrix} = \begin{pmatrix} E_x \\ G_x \end{pmatrix} \cos \psi + \begin{pmatrix} 0 \\ \sqrt{E_y^2 - G_x^2} \end{pmatrix} \sin \psi. \quad (\text{A.21})$$

Note that Eqs. (A.19, A.20), which define the beam cross section, are the result of a many particle treatment due to the averaging process as described in Eq. (A.10) (see Refs. [5–7]).

Lastly, we can rewrite  $\tan 2\theta_p$  as:

$$\begin{aligned} \sin \theta_p &= \text{sgn}\{(E_x^2 - E_y^2)E_x G_x\} \sqrt{\frac{1}{2}(1 - \cos 2\theta_p)} \\ \cos \theta_p &= \sqrt{\frac{1}{2}(1 + \cos 2\theta_p)} \end{aligned} \quad (\text{A.22})$$

### Coupling angle in the physical $X - Y$ plane

Although the coupling angle is defined for a multi-particle system it is instructive to relate it to the physical plane ( $X - Y$ ) of single particle motion. In this plane motion

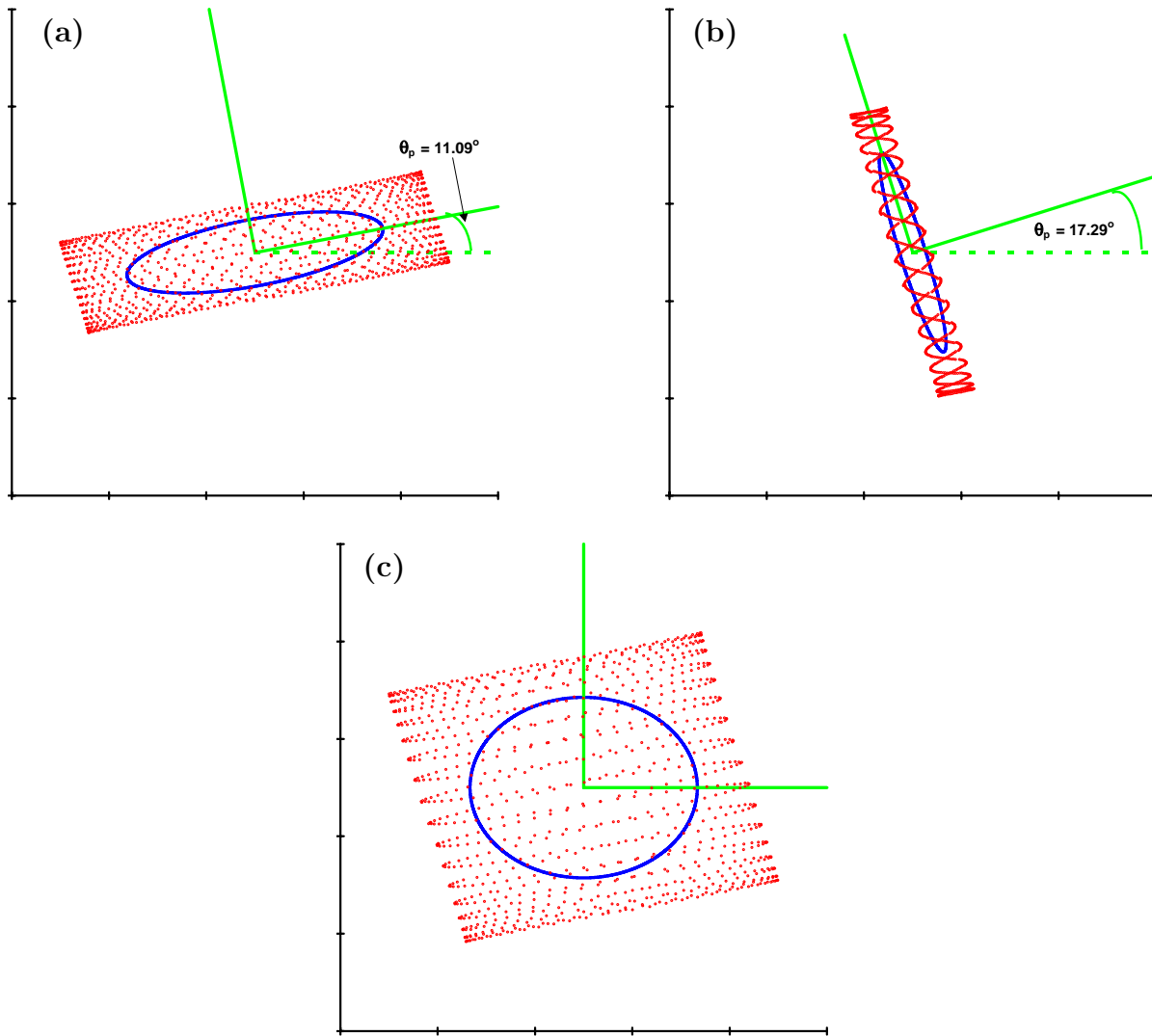


Figure 3: Numerical calculation of the single particle motion in the  $(X - Y)$ -plane. The action ratios between horizontal and vertical motion planes are 1:10, 10:1 and 1:1 in part (a), (b) and (c), respectively. The angle  $\theta_p$  is given in degrees. The ellipse represents the cross section of the averaged  $(\bar{X} - \bar{Y})$ -plane.

is restricted to a parallelogram which is tilted due to the linear coupling. Numerical simulations were carried out for a FODO structure including considerable skew quadrupole components. Three particles have been tracked over 1000 turns, for mainly horizontal motion, mainly vertical motion and for a  $J_I = J_{II}$  beam in Figure 3 (a), (b) and (c), respectively. In the limit of one dominant plane of motion (see (a) or (b)) the calculated coupling angle is the angle by which the longer side of the parallelogram is tilted. For the intermediate case the coupling angle goes to zero when the ellipse approaches the circle, see Figure 3 (c).

Note that a zero coupling angle does not imply that the motion is decoupled but instead it means that the eigenplanes are not tilted with respect to the uncoupled case.

## Appendix B: Synchro-Beam Mapping within Solenoid Fields

The synchro-beam map is described by Eq. (2.53), it consists of a transformation from the IP to the CP, followed by the beam-beam kick and the backwards transformation to the IP. In this appendix the transformation  $D(S)$  from the IP to the CP is generalised to include solenoid fields. For a particle within a solenoid field one obtains in linear approximation in  $S$ :

$$\begin{aligned}\bar{x}^* &= x^* + S \frac{\partial \mathcal{H}}{\partial p_x^*}; & \bar{p}_x^* &= p_x^* - S \frac{\partial \mathcal{H}}{\partial x^*}; \\ \bar{y}^* &= y^* + S \frac{\partial \mathcal{H}}{\partial p_y^*}; & \bar{p}_y^* &= p_y^* - S \frac{\partial \mathcal{H}}{\partial y^*}; \\ \bar{z}^* &= z^* + S \frac{\partial \mathcal{H}}{\partial p_z^*}; & \bar{p}_z^* &= p_z^* - S \frac{\partial \mathcal{H}}{\partial z^*}\end{aligned}\tag{B.1}$$

with  $S$  given by Eq. (2.46)

$$S = S(z^*, Z^\dagger) = \frac{z^* - Z^\dagger}{2}.\tag{B.2}$$

The normal coordinates are taken at the interaction point while the barred coordinates are taken at the collision point. In the following we skip the symbol ‘\*’ which indicates the Lorentz transformation of the coordinates of the test particle. Note that we temporarily ignore the contribution of the strong beam (see Eq. (2.51)).

It is most convenient to symplectify Eq. (B.1) such that the total SBM-transformation is symplectic by definition. In the following, three methods of symplectification shall be described and applied by using the Hamiltonian of a solenoid field. The last method is evaluated for arbitrary energies.

### 1. Generating Function

We introduce the generating function

$$F_2(x, \bar{p}_x; y, \bar{p}_y; z, \bar{p}_z) = x\bar{p}_x + y\bar{p}_y + z\bar{p}_z + S\mathcal{H}(x, \bar{p}_x; y, \bar{p}_y; z, \bar{p}_z)\tag{B.3}$$

in analogy to the method applied by E. Forest and K. Ohmi for the symplectic integration of complex wigglers [8, 9]. The transformation equations due to  $F_2$  take the form:

$$\begin{aligned}\bar{x} &= \frac{\partial F_2}{\partial \bar{p}_x} = x + S \frac{\partial \mathcal{H}}{\partial \bar{p}_x}; & p_x &= \frac{\partial F_2}{\partial x} = \bar{p}_x + S \frac{\partial \mathcal{H}}{\partial x}; \\ \bar{y} &= \frac{\partial F_2}{\partial \bar{p}_y} = y + S \frac{\partial \mathcal{H}}{\partial \bar{p}_y}; & p_y &= \frac{\partial F_2}{\partial y} = \bar{p}_y + S \frac{\partial \mathcal{H}}{\partial y}; \\ \bar{z} &= \frac{\partial F_2}{\partial \bar{p}_z} = z + S \frac{\partial \mathcal{H}}{\partial \bar{p}_z}; & p_z &= \frac{\partial F_2}{\partial z} = \bar{p}_z + \frac{1}{2}\mathcal{H} + S \frac{\partial \mathcal{H}}{\partial z}.\end{aligned}\tag{B.4}$$

For a solenoid field (with strength  $H$ ) the Hamiltonian reads:

$$\mathcal{H}(x, p_x; y, p_y; z, p_z) = \frac{1}{2} \{ [p_x + yH]^2 + [p_y - xH]^2 \}.\tag{B.5}$$

The corresponding generating function is

$$F_2(x, \bar{p}_x; y, \bar{p}_y; z, \bar{p}_z) = x\bar{p}_x + y\bar{p}_y + z\bar{p}_z + \frac{S}{2} \{ [\bar{p}_x + yH]^2 + [\bar{p}_y - xH]^2 \}.\tag{B.6}$$

Thus:

$$\begin{aligned}
\bar{x} &= \frac{\partial F_2}{\partial \bar{p}_x} = x + S[\bar{p}_x + yH]; & p_x &= \frac{\partial F_2}{\partial x} = \bar{p}_x - S[\bar{p}_y - xH]H; \\
\bar{y} &= \frac{\partial F_2}{\partial \bar{p}_y} = y + S[\bar{p}_y - xH]; & p_y &= \frac{\partial F_2}{\partial y} = \bar{p}_y + S[\bar{p}_x + yH]H; \\
\bar{z} &= \frac{\partial F_2}{\partial \bar{p}_z} = z; & p_z &= \frac{\partial F_2}{\partial z} = \bar{p}_z + \frac{1}{4} \{[\bar{p}_x + yH]^2 + [\bar{p}_y - xH]^2\}.
\end{aligned} \tag{B.7}$$

From Eqs. (B.7) we get:

$$\begin{aligned}
\bar{x} - S\bar{p}_x &= x + SyH; & \bar{p}_x - S\bar{p}_yH &= p_x - SxH^2; \\
\bar{y} - S\bar{p}_y &= y - SxH; & \bar{p}_y + S\bar{p}_xH &= p_y - SyH^2
\end{aligned} \tag{B.8}$$

or

$$\begin{pmatrix} 1 & -S & 0 & 0 \\ 0 & 1 & 0 & -SH \\ 0 & 0 & 1 & -S \\ 0 & SH & 0 & 1 \end{pmatrix} \begin{pmatrix} \bar{x} \\ \bar{p}_x \\ \bar{y} \\ \bar{p}_y \end{pmatrix} = \begin{pmatrix} 1 & 0 & SH & 0 \\ -SH^2 & 1 & 0 & 0 \\ -SH & 0 & 1 & 0 \\ 0 & 0 & -SH^2 & 1 \end{pmatrix} \begin{pmatrix} x \\ p_x \\ y \\ p_y \end{pmatrix}. \tag{B.9}$$

Using the relation:

$$\begin{pmatrix} 1 & -S & 0 & 0 \\ 0 & 1 & 0 & -SH \\ 0 & 0 & 1 & -S \\ 0 & SH & 0 & 1 \end{pmatrix}^{-1} = \frac{1}{1 + (SH)^2} \begin{pmatrix} 1 + S^2 & S & 0 & S^2H \\ 0 & 1 & 0 & SH \\ 0 & -S^2H & 1 + (SH)^2 & S \\ 0 & -SH & 0 & 1 \end{pmatrix} \tag{B.10}$$

we obtain from (B.9):

$$\begin{pmatrix} \bar{x} \\ \bar{p}_x \\ \bar{y} \\ \bar{p}_y \end{pmatrix} = \frac{1}{1 + (SH)^2} \begin{pmatrix} 1 & S & SH & S^2H \\ -SH^2 & 1 & -S^2H^3 & SH \\ -SH & -S^2H & 1 & S \\ S^2H^3 & -SH & -SH^2 & 1 \end{pmatrix} \begin{pmatrix} x \\ p_x \\ y \\ p_y \end{pmatrix}, \tag{B.11}$$

in particular we have:

$$\begin{aligned}
\bar{p}_x + yH &= \frac{1}{1 + (SH)^2} \{SH[p_y - xH] + [p_x + yH]\}; \\
\bar{p}_y - xH &= \frac{1}{1 + (SH)^2} \{-SH[p_x + yH] + [p_y - xH]\}.
\end{aligned} \tag{B.12}$$

Inserting Eqs. (B.12) into (B.7), we finally get:

$$\bar{p}_z = p_z - \frac{1}{4} \frac{1}{1 + (SH)^2} \{[p_x + yH]^2 + [p_y - xH]^2\}. \tag{B.13}$$

Note that  $z$  remains unchanged (see Eq. (B.7)).

Remark:

For  $H = 0$  (drift space), we obtain from Eqs. (B.7), (B.11) and (B.13) the transformation equations:

$$\begin{aligned}\bar{x} &= x + Sp_x; & \bar{p}_x &= p_x; \\ \bar{y} &= y + Sp_y; & \bar{p}_y &= p_y; \\ \bar{z} &= z; & \bar{p}_z &= p_z - \frac{1}{4}(p_x^2 + p_y^2)\end{aligned}\tag{B.14}$$

which are the same as Eqs. (2.51, 2.52) without the extra terms due to the strong beam.

## 2. Lie Series

In the following we again skip the symbol ‘\*’ which indicates the Lorentz transformation of the coordinates of the test particle. The canonical equations of motion:

$$\begin{aligned}\frac{dx}{ds} &= \frac{\partial \mathcal{H}}{\partial p_x}; & \frac{dp_x}{ds} &= -\frac{\partial \mathcal{H}}{\partial x}; \\ \frac{dy}{ds} &= \frac{\partial \mathcal{H}}{\partial p_y}; & \frac{dp_y}{ds} &= -\frac{\partial \mathcal{H}}{\partial y}; \\ \frac{dz}{ds} &= \frac{\partial \mathcal{H}}{\partial p_z}; & \frac{dp_z}{ds} &= -\frac{\partial \mathcal{H}}{\partial z}\end{aligned}\tag{B.15}$$

due to a Hamiltonian

$$\mathcal{H}(\vec{x}) = \mathcal{H}(x, p_x, y, p_y, z, p_z)\tag{B.16}$$

can be integrated by Lie-series [10, 11]:

$$\vec{x}(s) = \exp[(s - s_0)D]\vec{x}\tag{B.17}$$

with

$$\begin{aligned}\vec{x} &= (x, p_x, y, p_y, z, p_z)^T; \\ \vec{\bar{x}} &= (\bar{x}, \bar{p}_x, \bar{y}, \bar{p}_y, \bar{z}, \bar{p}_z)^T;\end{aligned}\tag{B.18}$$

$$\vec{x} \equiv \vec{x}(s_0)$$

and

$$\begin{aligned}D &= \left[ \frac{\partial}{\partial p_x} \mathcal{H}(\vec{x}) \right] \frac{\partial}{\partial x} - \left[ \frac{\partial}{\partial x} \mathcal{H}(\vec{x}) \right] \frac{\partial}{\partial p_x} \\ &+ \left[ \frac{\partial}{\partial p_y} \mathcal{H}(\vec{x}) \right] \frac{\partial}{\partial y} - \left[ \frac{\partial}{\partial y} \mathcal{H}(\vec{x}) \right] \frac{\partial}{\partial p_y} \\ &+ \left[ \frac{\partial}{\partial p_z} \mathcal{H}(\vec{x}) \right] \frac{\partial}{\partial z} - \left[ \frac{\partial}{\partial z} \mathcal{H}(\vec{x}) \right] \frac{\partial}{\partial p_z}.\end{aligned}\tag{B.19}$$

In particular we get for the map from the interaction point (IP) to the collision point (CP)  $s_{CP} = s_{IP} + S$ :

$$\vec{\bar{x}}(s_{CP}) = \exp[SD]\vec{x}; \quad \vec{x} \equiv \vec{x}(s_{IP})\tag{B.20}$$

which is not symplectic in general due to the factor  $S$ .  
In order to symplectify Eq. (B.20), we introduce a new Hamiltonian

$$\mathcal{H}_{SBM}(\vec{x}) = S\mathcal{H}(\vec{x}) \quad (\text{B.21})$$

by modifying the longitudinal coordinates of motion, leading to the canonical map:

$$\vec{x}(s_{CP}) = \exp[D_{SBM}] \vec{x} \quad (\text{B.22})$$

with

$$\begin{aligned} D_{SBM} &= \left[ \frac{\partial}{\partial p_x} \mathcal{H}_{SBM}(\vec{x}) \right] \frac{\partial}{\partial x} - \left[ \frac{\partial}{\partial x} \mathcal{H}_{SBM}(\vec{x}) \right] \frac{\partial}{\partial p_x} \\ &+ \left[ \frac{\partial}{\partial p_y} \mathcal{H}_{SBM}(\vec{x}) \right] \frac{\partial}{\partial y} - \left[ \frac{\partial}{\partial y} \mathcal{H}_{SBM}(\vec{x}) \right] \frac{\partial}{\partial p_y} \\ &+ \left[ \frac{\partial}{\partial p_z} \mathcal{H}_{SBM}(\vec{x}) \right] \frac{\partial}{\partial z} - \left[ \frac{\partial}{\partial z} \mathcal{H}_{SBM}(\vec{x}) \right] \frac{\partial}{\partial p_z} \\ &= SD - \frac{1}{2} \mathcal{H}(\vec{x}) \frac{\partial}{\partial p_z} \end{aligned} \quad (\text{B.23})$$

and  $D$  given by Eq. (B.19).  
Using the Hamiltonian

$$\mathcal{H}(\vec{x}) = \frac{1}{2} \{ [p_x + yH]^2 + [p_y - xH]^2 \} \quad (\text{B.24})$$

of a solenoid, we obtain:

$$\begin{aligned} D &= [p_x + yH] \frac{\partial}{\partial x} + [p_y - xH] H \frac{\partial}{\partial p_x} \\ &+ [p_y - xH] \frac{\partial}{\partial y} - [p_x + yH] H \frac{\partial}{\partial p_y}; \\ D_{SBM} &= SD - \frac{1}{4} \{ [p_x + yH]^2 + [p_y - xH]^2 \} \frac{\partial}{\partial p_z}. \end{aligned} \quad (\text{B.25})$$

For the longitudinal coordinates we then get:

$$\begin{aligned} D_{SBM} z &= SDz = 0; \\ [D_{SBM}]^\nu z &= 0 \quad \text{for } \nu \in \mathbb{N} \end{aligned} \quad (\text{B.26})$$

resulting in

$$\{ \exp[D_{SBM}] \} z = z \quad (\text{B.27})$$



and

$$\begin{aligned}
D_{SBM} p_z &= -\frac{1}{2}\mathcal{H}(\vec{x}) \\
&= -\frac{1}{4}\{[p_x + yH]^2 + [p_y - xH]^2\};
\end{aligned} \tag{B.28}$$

$$[D_{SBM}]^2 p_z = -\frac{1}{2}SD\mathcal{H}(\vec{x}) = 0;$$

$$[D_{SBM}]^\nu p_z = 0 \quad \text{for } \nu > 1;$$

$$\implies \{\exp[D_{SBM}]\} p_z = p_z - \frac{1}{4}\{[p_x + yH]^2 + [p_y - xH]^2\}. \tag{B.29}$$

For the transverse coordinates we have:

$$\begin{aligned}
D_{SBM} \begin{pmatrix} x \\ p_x \\ y \\ p_y \end{pmatrix} &= SD \begin{pmatrix} x \\ p_x \\ y \\ p_y \end{pmatrix} = S \begin{pmatrix} p_x + yH \\ p_y H - xH^2 \\ p_y - xH \\ -p_x H - yH^2 \end{pmatrix} \\
&= S \underbrace{\begin{pmatrix} 0 & 1 & H & 0 \\ -H^2 & 0 & 0 & H \\ -H & 0 & 0 & 1 \\ 0 & -H & -H^2 & 0 \end{pmatrix}}_{\underline{C}} \begin{pmatrix} x \\ p_x \\ y \\ p_y \end{pmatrix};
\end{aligned} \tag{B.30}$$

$$[D_{SBM}]^\nu \begin{pmatrix} x \\ p_x \\ y \\ p_y \end{pmatrix} = S^\nu \quad D^\nu \begin{pmatrix} x \\ p_x \\ y \\ p_y \end{pmatrix} = S^\nu \underline{C}^\nu \begin{pmatrix} x \\ p_x \\ y \\ p_y \end{pmatrix}; \tag{B.31}$$

$$\implies \{\exp[D_{SBM}]\} \begin{pmatrix} x \\ p_x \\ y \\ p_y \end{pmatrix} = \{\exp[S\underline{C}]\} \begin{pmatrix} x \\ p_x \\ y \\ p_y \end{pmatrix}.$$

In order to calculate  $\exp[S\underline{C}]$ , we write:

$$\underline{C} = \underline{C}_1 + \underline{C}_2 \tag{B.32}$$

with

$$\underline{C}_1 = \begin{pmatrix} 0 & 1 & 0 & 0 \\ -H^2 & 0 & 0 & 0 \\ 0 & 0 & 0 & 1 \\ 0 & 0 & -H^2 & 0 \end{pmatrix}; \quad \underline{C}_2 = H \begin{pmatrix} 0 & 0 & 1 & 0 \\ 0 & 0 & 0 & 1 \\ -1 & 0 & 0 & 0 \\ 0 & -1 & 0 & 0 \end{pmatrix} \tag{B.33}$$

and

$$\underline{C}_1 \cdot \underline{C}_2 = \underline{C}_2 \cdot \underline{C}_1 \tag{B.34}$$

$$\implies \exp[S\underline{C}] = \exp[S\underline{C}_1] \cdot \exp[S\underline{C}_2].$$

Furthermore we obtain:

$$\begin{aligned}
[\underline{C}_1]^{2n} &= (-1)^n H^{2n} \underline{I}; \\
[\underline{C}_1]^{2n+1} &= (-1)^n H^{2n} \underline{C}_1 \\
&= (-1)^n H^{2n+1} \begin{pmatrix} 0 & 1/H & 0 & 0 \\ -H & 0 & 0 & 0 \\ 0 & 0 & 0 & 1/H \\ 0 & 0 & -H & 0 \end{pmatrix}
\end{aligned} \tag{B.35}$$

(with  $\underline{I}$  an  $4 \times 4$  unity matrix) and thus:

$$\begin{aligned}
\exp[SC_1] &= \sum_{n=0}^{\infty} \frac{1}{(2n)!} (-1)^n (\Delta\theta)^{2n} \underline{I} \\
&+ \sum_{n=0}^{\infty} \frac{1}{(2n+1)!} (-1)^n (\Delta\theta)^{2n+1} \begin{pmatrix} 0 & 1/H & 0 & 0 \\ -H & 0 & 0 & 0 \\ 0 & 0 & 0 & 1/H \\ 0 & 0 & -H & 0 \end{pmatrix} \\
&= \underline{I} \cos \Delta\theta + \begin{pmatrix} 0 & 1/H & 0 & 0 \\ -H & 0 & 0 & 0 \\ 0 & 0 & 0 & 1/H \\ 0 & 0 & -H & 0 \end{pmatrix} \sin \Delta\theta.
\end{aligned} \tag{B.36}$$

resulting in:

$$\exp[SC_1] = \begin{pmatrix} \cos \Delta\theta & \frac{\sin \Delta\theta}{H} & 0 & 0 \\ -H \sin \Delta\theta & \cos \Delta\theta & 0 & 0 \\ 0 & 0 & \cos \Delta\theta & \frac{\sin \Delta\theta}{H} \\ 0 & 0 & -H \sin \Delta\theta & \cos \Delta\theta \end{pmatrix} \tag{B.37}$$

with  $\Delta\theta = SH$ .

In a similar way one can derive:

$$\begin{aligned}
[\underline{C}_2]^{2n} &= (-1)^n H^{2n} \underline{I}; \\
[\underline{C}_2]^{2n+1} &= (-1)^n H^{2n+1} \left[ \frac{1}{H} \underline{C}_2 \right]
\end{aligned} \tag{B.38}$$

$$\begin{aligned}
\implies \exp[SC_2] &= \underline{I} \cos \Delta\theta + \left[ \frac{1}{H} \underline{C}_2 \right] \sin \Delta\theta \\
&= \begin{pmatrix} \cos \Delta\theta & 0 & \sin \Delta\theta & 0 \\ 0 & \cos \Delta\theta & 0 & \sin \Delta\theta \\ -\sin \Delta\theta & 0 & \cos \Delta\theta & 0 \\ 0 & -\sin \Delta\theta & 0 & \cos \Delta\theta \end{pmatrix}.
\end{aligned} \tag{B.39}$$

Inserting Eqs. (B.37) and (B.39) into Eq. (B.34), we finally obtain (see Eq. (B.31)):

$$\begin{aligned} \begin{pmatrix} \bar{x} \\ \bar{p}_x \\ \bar{y} \\ \bar{p}_y \end{pmatrix} &= \{\exp[D_{SBM}]\} \begin{pmatrix} x \\ p_x \\ y \\ p_y \end{pmatrix} = \begin{pmatrix} \cos \Delta\theta & \frac{\sin \Delta\theta}{H} & 0 & 0 \\ -H \sin \Delta\theta & \cos \Delta\theta & 0 & 0 \\ 0 & 0 & \cos \Delta\theta & \frac{\sin \Delta\theta}{H} \\ 0 & 0 & -H \sin \Delta\theta & \cos \Delta\theta \end{pmatrix} \times \\ &\begin{pmatrix} \cos \Delta\theta & 0 & \sin \Delta\theta & 0 \\ 0 & \cos \Delta\theta & 0 & \sin \Delta\theta \\ -\sin \Delta\theta & 0 & \cos \Delta\theta & 0 \\ 0 & -\sin \Delta\theta & 0 & \cos \Delta\theta \end{pmatrix} \begin{pmatrix} x \\ p_x \\ y \\ p_y \end{pmatrix}. \end{aligned} \quad (\text{B.40})$$

Eq. (B.11) and Eq. (B.40) are both symplectic approximations of the solenoid kick. The approximations agree in first-order with respect to  $\Delta\theta = SH$ . In particular, in the limit of  $H = 0$ , which represents a drift space, they give the same results (see Eq. (B.14)).

### 3. Integration method

Moreover, we will generalise the function for arbitrary energy. The map  $\vec{x}(s_{IP}) \rightarrow \vec{x}(s_{CP})$  can also be obtained by introducing an artificial parameter  $\tau$  and solving the canonical equations of motion

$$\vec{x}' \equiv \frac{d}{d\tau} \vec{x} = -\underline{J} \frac{\partial}{\partial \vec{x}} \mathcal{H}_{SBM} \quad (\text{B.41})$$

for  $\Delta\tau = 1$  with  $\underline{J}$  given by (A.6) (see Eqs. (B.17), (B.22)).

We demonstrate this by using the new Hamiltonian (again denoted by  $\mathcal{H}$ )

$$\mathcal{H} = \frac{\mathcal{H}_0(x, p_x, y, p_y)}{[1 + p_z]}, \quad (\text{B.42})$$

with

$$\mathcal{H}_0(x, p_x; y, p_y) = \frac{1}{2} \{ [p_x + yH]^2 + [p_y - xH]^2 \}. \quad (\text{B.43})$$

generalising thus the Hamiltonian  $\mathcal{H}$  in Eqs. (B.5) and (B.24) by taking into account an arbitrary energy of the particles (due to the denominator  $[1 + p_z]$  in Eq. (B.42)). Then we have:

$$\mathcal{H}_{SBM} = S \frac{\mathcal{H}_0(x, p_x, y, p_y)}{[1 + p_z]} \quad (\text{B.44})$$

leading to the equations of motion:

$$\begin{aligned}
x' &= \frac{\partial \mathcal{H}_{SBM}}{\partial p_x} = S \frac{[p_x + yH]}{[1 + p_z]}, \\
p'_x &= -\frac{\partial \mathcal{H}_{SBM}}{\partial x} = S \frac{[p_y - xH]H}{[1 + p_z]}, \\
y' &= \frac{\partial \mathcal{H}_{SBM}}{\partial p_y} = S \frac{[p_y - xH]}{[1 + p_z]}, \\
p'_y &= -\frac{\partial \mathcal{H}_{SBM}}{\partial y} = -S \frac{[p_x + yH]H}{[1 + p_z]}, \\
z' &= \frac{\partial \mathcal{H}_{SBM}}{\partial p_z} = -\frac{S}{2} \frac{[p_x + yH]^2 + [p_y - xH]^2}{[1 + p_z]^2}, \\
p'_z &= -\frac{\partial \mathcal{H}_{SBM}}{\partial z} = -\frac{1}{4} \frac{[p_x + yH]^2 + [p_y - xH]^2}{[1 + p_z]}.
\end{aligned} \tag{B.45}$$

From Eqs. (B.45) we get

$$\begin{aligned}
\frac{d}{d\tau} \mathcal{H}_0(x, p_x, y, p_y) &= \frac{\partial \mathcal{H}_0}{\partial x} x' + \frac{\partial \mathcal{H}_0}{\partial p_x} p'_x + \frac{\partial \mathcal{H}_0}{\partial y} y' + \frac{\partial \mathcal{H}_0}{\partial p_y} p'_y \\
&= \frac{\partial \mathcal{H}_0}{\partial x} \frac{\partial \mathcal{H}_{SBM}}{\partial p_x} - \frac{\partial \mathcal{H}_0}{\partial p_x} \frac{\partial \mathcal{H}_{SBM}}{\partial x} + \frac{\partial \mathcal{H}_0}{\partial y} \frac{\partial \mathcal{H}_{SBM}}{\partial p_y} - \frac{\partial \mathcal{H}_0}{\partial p_y} \frac{\partial \mathcal{H}_{SBM}}{\partial y} \\
&= S \frac{1}{[1 + p_z]} \left\{ \frac{\partial \mathcal{H}_0}{\partial x} \frac{\partial \mathcal{H}_0}{\partial p_x} - \frac{\partial \mathcal{H}_0}{\partial p_x} \frac{\partial \mathcal{H}_0}{\partial x} + \frac{\partial \mathcal{H}_0}{\partial y} \frac{\partial \mathcal{H}_0}{\partial p_y} - \frac{\partial \mathcal{H}_0}{\partial p_y} \frac{\partial \mathcal{H}_0}{\partial y} \right\} \\
&= 0; \\
&\implies \mathcal{H}_0(x, p_x, y, p_y) = \text{const.}
\end{aligned} \tag{B.46}$$

Thus Eq. (B.45) takes the initial value

$$p'_z = -\frac{1}{2} \frac{\mathcal{H}_0(x, p_x, y, p_y)}{[1 + p_z]} \tag{B.47}$$

with the solution

$$\begin{aligned}
\bar{p}_z(\tau) &= [1 + p_z] \sqrt{1 - \frac{1}{2} \frac{\mathcal{H}_0(x, p_x, y, p_y)}{[1 + p_z]^2} \tau - 1} \\
\implies \bar{p}_z &= [1 + p_z] \sqrt{1 - \frac{1}{2} \frac{\mathcal{H}_0(x, p_x, y, p_y)}{[1 + p_z]^2} - 1}
\end{aligned} \tag{B.48}$$

where we have used

$$\begin{aligned}
p_z &\equiv p_z(0); \\
\bar{p}_z &\equiv p_z(1).
\end{aligned} \tag{B.49}$$

From Eqs. (B.45) we obtain

$$\begin{aligned}
\frac{d}{d\tau} \frac{z - Z^\dagger}{[1 + p_z]} &= \frac{z'(1 + p_z) - (z - Z^\dagger)p'_z}{[1 + p_z]^2} \\
&= \frac{1}{[1 + p_z]^2} \left\{ -\frac{z - Z^\dagger}{4} \frac{[p_x + yH]^2 + [p_y - xH]^2}{[1 + p_z]} \right. \\
&\quad \left. + \frac{z - Z^\dagger}{4} \frac{[p_x + yH]^2 + [p_y - xH]^2}{[1 + p_z]} \right\} \\
&= 0; \\
\implies \frac{\bar{z} - Z^\dagger}{[1 + p_z]} &= \frac{z(0) - Z^\dagger}{[1 + p_z(0)]} \equiv \frac{z - Z^\dagger}{[1 + p_z]}
\end{aligned} \tag{B.50}$$

and thus after the synchro-beam mapping we get:

$$\bar{z} - Z^\dagger = (z - Z^\dagger) \sqrt{1 - \frac{1}{2} \frac{\mathcal{H}_0(x, p_x, y, p_y)}{[1 + p_z]^2}}. \tag{B.51}$$

Finally Eqs. (B.45) can be written as

$$\begin{aligned}
x' &= \frac{1}{2} \frac{z - Z^\dagger}{[1 + p_z]} [p_x + yH]; & p'_x &= \frac{1}{2} \frac{z - Z^\dagger}{[1 + p_z]} [p_y - xH]H; \\
y' &= \frac{1}{2} \frac{z - Z^\dagger}{[1 + p_z]} [p_y - xH]; & p'_y &= -\frac{1}{2} \frac{z - Z^\dagger}{[1 + p_z]} [p_x + yH]H
\end{aligned} \tag{B.52}$$

leading again to Eq. (B.40) for  $\Delta\tau = 1$  and  $\Delta\theta = SH/(1 + p_z)$ .

### Appendix C: Linear Beam-Beam model

In this appendix we derive the linear beam-beam model for a single slice. Using Eq. (1.1) for the whole bunch at the IP, we can write (using Eq. (2.4)):

$$\begin{aligned}
p_x &= -N^* \frac{\partial}{\partial x} U(\hat{x}, \hat{y}; \hat{\Sigma}_{11}, \hat{\Sigma}_{33}) \\
&= -N^* \left\{ \cos \theta \frac{\partial}{\partial \hat{x}} U(\hat{x}, \hat{y}; \hat{\Sigma}_{11}, \hat{\Sigma}_{33}) - \sin \theta \frac{\partial}{\partial \hat{y}} U(\hat{x}, \hat{y}; \hat{\Sigma}_{11}, \hat{\Sigma}_{33}) \right\};
\end{aligned} \tag{C.1}$$

$$\begin{aligned}
p_y &= -N^* \frac{\partial}{\partial y} U(\hat{x}, \hat{y}; \hat{\Sigma}_{11}, \hat{\Sigma}_{33}) \\
&= -N^* \left\{ \sin \theta \frac{\partial}{\partial \hat{x}} U(\hat{x}, \hat{y}; \hat{\Sigma}_{11}, \hat{\Sigma}_{33}) + \cos \theta \frac{\partial}{\partial \hat{y}} U(\hat{x}, \hat{y}; \hat{\Sigma}_{11}, \hat{\Sigma}_{33}) \right\}.
\end{aligned}$$

For small values

$$\hat{x}^2 \ll \hat{\Sigma}_{11} ; \hat{y}^2 \ll \hat{\Sigma}_{33} \tag{C.2}$$

the behaviour is linear [12]:

$$\begin{aligned}
N^* \frac{\partial}{\partial \hat{x}} U(\hat{x}, \hat{y}; \hat{\Sigma}_{11}, \hat{\Sigma}_{33}) &= \frac{1}{f_1} \hat{x}; \\
N^* \frac{\partial}{\partial \hat{y}} U(\hat{x}, \hat{y}; \hat{\Sigma}_{11}, \hat{\Sigma}_{33}) &= \frac{1}{f_2} \hat{y}
\end{aligned} \tag{C.3}$$

with focal length  $f_1$  and  $f_2$  defined by

$$\begin{aligned}
\frac{1}{f_1} &= \frac{2N^* r_p}{\gamma_0 (E_1 + E_2) E_1}; \\
\frac{1}{f_2} &= \frac{2N^* r_p}{\gamma_0 (E_1 + E_2) E_2}
\end{aligned} \tag{C.4}$$

and with  $E_1$  and  $E_2$  taken from Appendix A (Eq. (A.16)). Thus:

$$\begin{aligned}
p_x &= -\hat{x} \frac{1}{f_1} \cos \theta + \hat{y} \frac{1}{f_2} \sin \theta \\
&= -\frac{1}{f_1} [x \cos \theta + y \sin \theta] \cos \theta + \frac{1}{f_2} [-x \sin \theta + y \cos \theta] \sin \theta \\
&= -\left( \frac{1}{f_1} \cos^2 \theta + \frac{1}{f_2} \sin^2 \theta \right) x - \frac{1}{2} \left( \frac{1}{f_1} - \frac{1}{f_2} \right) y \sin 2\theta; \\
p_y &= -\hat{x} \frac{1}{f_1} \sin \theta - \hat{y} \frac{1}{f_2} \cos \theta \\
&= -\frac{1}{f_1} [x \cos \theta + y \sin \theta] \sin \theta - \frac{1}{f_2} [-x \sin \theta + y \cos \theta] \cos \theta \\
&= -\frac{1}{2} \left( \frac{1}{f_1} - \frac{1}{f_2} \right) x \sin 2\theta - \left( \frac{1}{f_1} \sin^2 \theta + \frac{1}{f_2} \cos^2 \theta \right) y.
\end{aligned} \tag{C.5}$$

In matrix form we may write:

$$\vec{x}(s_{IP} + 0) = \underline{T}_{bb}\vec{x}(s_{IP} - 0) \quad (\text{C.6})$$

with

$$\underline{T}_{bb} = \begin{pmatrix} 1 & 0 & 0 & 0 & 0 & 0 \\ -F_1 & 1 & -F & 0 & 0 & 0 \\ 0 & 0 & 1 & 0 & 0 & 0 \\ -F & 0 & -F_2 & 1 & 0 & 0 \\ 0 & 0 & 0 & 0 & 1 & 0 \\ 0 & 0 & 0 & 0 & 0 & 1 \end{pmatrix} \quad (\text{C.7})$$

and

$$\begin{aligned} F_1 &= \frac{1}{f_1} \cos^2 \theta + \frac{1}{f_2} \sin^2 \theta; \\ F_2 &= \frac{1}{f_1} \sin^2 \theta + \frac{1}{f_2} \cos^2 \theta; \\ F &= \frac{1}{2} \left( \frac{1}{f_1} - \frac{1}{f_2} \right) \sin 2\theta. \end{aligned} \quad (\text{C.8})$$

The equations of motion (C.6) can be obtained from the Hamiltonian

$$\mathcal{H}_{bb} = \left\{ \frac{1}{2} F_1 x^2 + \frac{1}{2} F_2 y^2 + F xy \right\} \delta(s - s_{IP}). \quad (\text{C.9})$$

Note that  $\underline{T}_{bb}$  in (C.7) contains quadrupole components ( $F_1$  and  $F_2$ ), focusing in both transverse planes. In addition there appears a skew quadrupole component ( $F$ ) resulting from the rotation angle  $\theta$  of the cross section due to the strong beam ( $F$  vanishes for  $\theta = 0$ ).

## Appendix D: Dispersion formalism including the beam-beam kick Canonical Transformation

The Hamiltonian for the whole ring consisting of bending magnets, quadrupoles, skew quadrupoles and solenoids, including the beam-beam kick in linear form, reads:

$$\mathcal{H} = \mathcal{H}_0 + \mathcal{H}_{bb} \quad (\text{D.1})$$

with [13, 14]

$$\begin{aligned} \mathcal{H}_0(x, y, z; p_x, p_y, p_z; s) &= \frac{1}{2} \frac{1}{\gamma_0^2} p_z^2 - [xK_x + yK_y]p_z \\ &+ \frac{1}{2} \{ [p_x + yH]^2 + [p_y - xH]^2 \} \\ &+ \frac{1}{2} \{ [K_x^2 + g] x^2 + [K_y^2 - g] y^2 - 2Nxy \} \\ &- \frac{1}{2} z^2 \frac{1}{\beta_0^2} \frac{eV(s)}{E_0} h \frac{2\pi}{L} \cos \varphi_{RF} \end{aligned} \quad (\text{D.2})$$

( $h$  is the harmonic number,  $V(s)$  is the RF voltage of the cavity and  $\varphi_{RF}$  is the RF phase) where the following abbreviations have been introduced:

$$\begin{aligned} g &= \frac{e}{p_0 c} \left( \frac{\partial \mathcal{B}_y}{\partial x} \right)_{x=z=0}; \\ N &= \frac{1}{2} \frac{e}{p_0 c} \left( \frac{\partial \mathcal{B}_x}{\partial x} - \frac{\partial \mathcal{B}_y}{\partial y} \right)_{x=z=0}; \\ H &= \frac{1}{2} \frac{e}{p_0 c} \mathcal{B}_s(0, 0, s); \\ K_x &= \frac{e}{p_0 c} \mathcal{B}_y(0, 0, s); \\ K_y &= -\frac{e}{p_0 c} \mathcal{B}_x(0, 0, s). \end{aligned} \quad (\text{D.3})$$

Note: the second term of the Hamiltonian is due to solenoid fields ( $H$ ) which have been treated in Appendix B.  $\mathcal{H}_{bb}$  is given by Eq. (C.9) in Appendix C. The Hamiltonian (D.1) then leads to the canonical equations of motion:



$$\begin{aligned}
\frac{d}{ds} x &= p_x + yH; \\
\frac{d}{ds} p_x &= p_z K_x - [K_x^2 + g]x + Ny \\
&\quad + [p_y - xH]H - [xF_1 + yF] \delta(s - s_{IP}); \\
\frac{d}{ds} y &= p_y - xH; \\
\frac{d}{ds} p_y &= p_z K_y - [K_y^2 - g]y + Nx \\
&\quad - [p_x + yH]H - [yF_2 + xF] \delta(s - s_{IP}); \\
\frac{d}{ds} z &= -[xK_x + yK_y] + \frac{1}{\gamma_0^2} p_z; \\
\frac{d}{ds} p_z &= \frac{1}{\beta_0^2} z \frac{eV(s)}{E_0} h \frac{2\pi}{L} \cos \varphi.
\end{aligned} \tag{D.4}$$

Note that the linear transverse betatron oscillations and the longitudinal motion (Eqs. (D.4)) are coupled by the terms

$$p_z K_x, \quad p_z K_y \quad \text{and} \quad -[xK_x + yK_y] \tag{D.5}$$

respectively, i.e. depending on the curvature of the orbit in the bending magnets.

In order to simplify these equations we introduce dispersion

$$\vec{D}(s) = \begin{pmatrix} D_1(s) \\ D_2(s) \\ D_3(s) \\ D_4(s) \end{pmatrix}; \tag{D.6}$$

$$\vec{D}(s) = \vec{D}(s + L).$$

New variables  $\tilde{x}$ ,  $\tilde{p}_x$ ,  $\tilde{y}$ ,  $\tilde{p}_y$ ,  $\tilde{z}$ ,  $\tilde{p}_z$  can be introduced which satisfy the dispersion relation:

$$\begin{aligned}
\tilde{x} &= x - p_z D_1; \\
\tilde{p}_x &= p_x - p_z D_2; \\
\tilde{y} &= y - p_z D_3; \\
\tilde{p}_y &= p_y - p_z D_4.
\end{aligned} \tag{D.7}$$

This replacement

$$(x, p_x, y, p_y, z, p_z) \longrightarrow (\tilde{x}, \tilde{p}_x, \tilde{y}, \tilde{p}_y, \tilde{z}, \tilde{p}_z) \tag{D.8}$$

can be achieved using the generating function [14–17]:

$$\begin{aligned}
F_2(x, y, z, \tilde{p}_x, \tilde{p}_y, \tilde{p}_z) &= \tilde{p}_x[x - \tilde{p}_z D_1] + \tilde{p}_z x D_2 \\
&+ \tilde{p}_y[y - \tilde{p}_z D_3] + \tilde{p}_z y D_4 \\
&- \frac{1}{2}[D_1 D_2 + D_3 D_4] \tilde{p}_z^2 + \tilde{p}_z z
\end{aligned} \tag{D.9}$$

with the result that:

$$\begin{aligned}
\tilde{x} &= \frac{\partial F_2}{\partial \tilde{p}_x} = x - \tilde{p}_z D_1; \\
p_x &= \frac{\partial F_2}{\partial x} = \tilde{p}_x + \tilde{p}_z D_2; \\
\tilde{y} &= \frac{\partial F_2}{\partial \tilde{p}_y} = y - \tilde{p}_z D_3; \\
p_y &= \frac{\partial F_2}{\partial y} = \tilde{p}_y + \tilde{p}_z D_4; \\
\tilde{z} &= \frac{\partial F_2}{\partial \tilde{p}_z} = z + [-\tilde{p}_x D_1 + x D_2 - \tilde{p}_y D_3 + y D_4] \\
&\quad - [D_1 D_2 + D_3 D_4] \tilde{p}_z
\end{aligned} \tag{D.10}$$

$$\begin{aligned}
&= z + \{-\tilde{p}_x D_1 + [x - D_1 \tilde{p}_z] D_2 \\
&\quad - \tilde{p}_y D_3 + [y - D_3 \tilde{p}_z] D_4\} \\
&= z + [-\tilde{p}_x D_1 + \tilde{x} D_2 - \tilde{p}_y D_3 + \tilde{y} D_4] \\
&= z + [-p_x D_1 + x D_2 - p_y D_3 + y D_4];
\end{aligned}$$

$$p_z = \frac{\partial F_2}{\partial z} = \tilde{p}_z$$

and

$$\tilde{\mathcal{H}} = \mathcal{H} + \frac{\partial F_2}{\partial s}. \tag{D.11}$$

In matrix form Eqs. (D.10) read :

$$\vec{\tilde{x}} = \underline{K}\vec{x}; \quad \vec{x} = \underline{K}^{-1}\vec{\tilde{x}}; \quad (\text{D.12})$$

with

$$\vec{\tilde{x}} = \begin{pmatrix} \tilde{x} \\ \tilde{p}_x \\ \tilde{y} \\ \tilde{p}_y \\ \tilde{z} \\ \tilde{p}_z \end{pmatrix} \quad (\text{D.13})$$

and

$$\underline{K}(s) = \begin{pmatrix} 1 & 0 & 0 & 0 & 0 & -D_1 \\ 0 & 1 & 0 & 0 & 0 & -D_2 \\ 0 & 0 & 1 & 0 & 0 & -D_3 \\ 0 & 0 & 0 & 1 & 0 & -D_4 \\ D_2 & -D_1 & D_4 & -D_3 & 1 & 0 \\ 0 & 0 & 0 & 0 & 0 & 1 \end{pmatrix}; \quad (\text{D.14})$$

$$\underline{K}^{-1}(s) = \begin{pmatrix} 1 & 0 & 0 & 0 & 0 & D_1 \\ 0 & 1 & 0 & 0 & 0 & D_2 \\ 0 & 0 & 1 & 0 & 0 & D_3 \\ 0 & 0 & 0 & 1 & 0 & D_4 \\ -D_2 & D_1 & -D_4 & D_3 & 1 & 0 \\ 0 & 0 & 0 & 0 & 0 & 1 \end{pmatrix}.$$

Note that  $\underline{K}(s)$  is symplectic:

$$\underline{K}^T(s)\underline{J}\underline{K}(s) = \underline{J} \quad (\text{D.15})$$

(with  $\underline{J}$  given by Eq. (A.6)).

Taking into account the defining equations for the dispersion in the general case of arbitrary velocity  $\beta_0$ :

$$\begin{aligned} \frac{d}{ds} D_1 &= D_2 + HD_3; \\ \frac{d}{ds} D_2 &= +[D_4 - HD_1]H - [K_x^2 + g]D_1 + ND_3 \\ &\quad - [F_1D_1 + FD_3] \delta(s - s_{IP}) + K_x; \\ \frac{d}{ds} D_3 &= D_4 - HD_1; \\ \frac{d}{ds} D_4 &= -[D_2 + HD_3]H + ND_1 - [K_y^2 - g]D_3 \\ &\quad - [F_1D_3 + FD_1] \delta(s - s_{IP}) + K_y, \end{aligned} \quad (\text{D.16})$$

the new Hamiltonian reads:

$$\begin{aligned}
\tilde{\mathcal{H}} &= \frac{1}{2} \{ [\tilde{p}_x + \tilde{y}H]^2 + [\tilde{p}_y - \tilde{x}H]^2 \} \\
&+ \frac{1}{2} \{ [K_x^2 + g]\tilde{x}^2 + [K_y^2 - g]\tilde{y}^2 \} - N\tilde{x}\tilde{y} \\
&- \frac{1}{2} [(K_x D_1 + K_y D_3) - 1/\gamma_0^2] \tilde{p}_z^2 \\
&- \frac{1}{\beta_0^2} h \frac{2\pi eV}{L E_0} \cos \varphi \times \frac{1}{2} \{ \tilde{z} + [\tilde{p}_x D_1 - \tilde{x}D_2 + \tilde{p}_y D_3 - \tilde{y}D_4] \}^2 \\
&+ \left[ \frac{1}{2} \tilde{x}^2 F_1 + \frac{1}{2} \tilde{y}^2 F_2 + Fxy \right] \delta(s - s_{IP}).
\end{aligned} \tag{D.17}$$

Note that the dispersion vector  $\vec{D}$  is the periodic solution of the linearised equations of orbital motion when the cavities are excluded and  $p_z = 1$ .

The coupling terms (see (D.5)) arising from the orbit curvature disappear. Instead, there is a term

$$-\frac{1}{2} \{ \tilde{z} + [\tilde{p}_x D_1 - \tilde{x}D_2 + \tilde{p}_y D_3 - \tilde{y}D_4] \}^2 \frac{1}{\beta_0^2} h \frac{2\pi eV}{L E_0} \cos \varphi$$

which disappears when all four dispersion terms ( $D_1, D_2, D_3, D_4$ ) are equal to zero at the location of the cavities.

For further analysis we split the Hamiltonian (D.17) into three parts:

$$\tilde{\mathcal{H}} = \tilde{\mathcal{H}}^0 + \tilde{\mathcal{H}}^1 + \tilde{\mathcal{H}}^2 \tag{D.18}$$

with

$$\begin{aligned}
\tilde{\mathcal{H}}^0 &= \frac{1}{2} \{ [\tilde{p}_x + \tilde{y}H]^2 + [\tilde{p}_y - \tilde{x}H]^2 \} \\
&+ \frac{1}{2} \{ [K_x^2 + g]\tilde{x}^2 + [K_y^2 - g]\tilde{y}^2 - N\tilde{x}\tilde{y} \} \\
&- \frac{1}{2} [(K_x D_1 + K_y D_3) - 1/\gamma_0^2] \tilde{p}_z^2 \\
&- \frac{1}{\beta_0^2} h \frac{2\pi eV}{L E_0} \cos \varphi \frac{1}{2} \tilde{z}^2;
\end{aligned} \tag{D.19}$$

$$\begin{aligned}
\tilde{\mathcal{H}}^1 &= -\frac{1}{\beta_0^2} h \frac{2\pi eV}{L E_0} \cos \varphi \times \\
&\frac{1}{2} [\tilde{p}_x D_1 - \tilde{x}D_2 + \tilde{p}_y D_3 - \tilde{y}D_4] \\
&\times \{ 2\tilde{z} + [\tilde{p}_x D_1 - \tilde{x}D_2 + \tilde{p}_y D_3 - \tilde{y}D_4] \};
\end{aligned}$$

$$\tilde{\mathcal{H}}^2 = \left[ \frac{1}{2} \tilde{x}^2 F_1 + \frac{1}{2} \tilde{y}^2 F_2 + Fxy \right] \delta(s - s_{IP}),$$

where we have gathered in  $\tilde{\mathcal{H}}^1$  all terms of the cavities producing synchro-betatron coupling and in  $\tilde{\mathcal{H}}^2$  the terms resulting from the beam-beam interaction.

In terms of the variables  $\tilde{x}$ ,  $\tilde{p}_x$ ,  $\tilde{y}$ ,  $\tilde{p}_y$ ,  $\tilde{z}$ ,  $\tilde{p}_z$ , Eq. (D.4) then takes the form :

$$\frac{d}{ds} \vec{\tilde{x}} = \underline{A}^{(0)} \vec{\tilde{x}} + \underline{A}^{(1)} \vec{\tilde{x}} + \underline{A}^{(2)} \vec{\tilde{x}} \quad (\text{D.20})$$

with

$$\begin{aligned} \underline{A}^{(0)} \vec{\tilde{x}} &= -J \frac{\partial \tilde{\mathcal{H}}^0}{\partial \vec{\tilde{x}}} \implies A_{mn}^{(0)} = -S_{ml} \frac{\partial^2 \tilde{\mathcal{H}}^0}{\partial y_l \partial y_n}; \\ \underline{A}^{(1)} \vec{\tilde{x}} &= -J \frac{\partial \tilde{\mathcal{H}}^1}{\partial \vec{\tilde{x}}} \implies A_{mn}^{(1)} = -S_{ml} \frac{\partial^2 \tilde{\mathcal{H}}^1}{\partial y_l \partial y_n}. \\ \underline{A}^{(2)} \vec{\tilde{x}} &= -J \frac{\partial \tilde{\mathcal{H}}^2}{\partial \vec{\tilde{x}}} \implies A_{mn}^{(2)} = -S_{ml} \frac{\partial^2 \tilde{\mathcal{H}}^2}{\partial y_l \partial y_n}. \end{aligned} \quad (\text{D.21})$$

In detail one obtains from Eqs. (D.19) :

$$\underline{A}^{(0)}(s) = \begin{pmatrix} \underline{A}_{4 \times 4}^{(\beta)}(s) & \underline{0}_{2 \times 2} \\ \underline{0}_{2 \times 4} & \underline{A}_{2 \times 2}^{(z)}(s) \end{pmatrix} \quad (\text{D.22})$$

$$\begin{aligned} \underline{A}^{(1)}(s) &= \frac{1}{\beta_0^2} \frac{eV(s)}{E_0} h \frac{2\pi}{L} \cos \varphi \\ &\times \begin{pmatrix} D_2 \vec{D} & -D_1 \vec{D} & D_4 \vec{D} & -D_3 \vec{D} & -\vec{D} & \vec{0}_4 \\ 0 & 0 & 0 & 0 & 0 & 0 \\ -D_2 & D_1 & -D_4 & D_3 & 0 & 0 \end{pmatrix} \end{aligned} \quad (\text{D.23})$$

$$\underline{A}^{(2)}(s) = \begin{pmatrix} 0 & 0 & 0 & 0 & 0 & 0 \\ -F_1 & 0 & -F & 0 & 0 & 0 \\ 0 & 0 & 0 & 0 & 0 & 0 \\ -F & 0 & -F_2 & 0 & 0 & 0 \\ 0 & 0 & 0 & 0 & 0 & 0 \\ 0 & 0 & 0 & 0 & 0 & 0 \end{pmatrix} \delta(s - s_{IP})$$

with

$$\underline{A}_{4 \times 4}^{(\beta)}(s) = \begin{pmatrix} 0 & 1 & H & 0 \\ -(K_x^2 + g + H^2) & 0 & N & H \\ -H & 0 & 0 & 1 \\ N & -H & -(K_y^2 - g + H^2) & 0 \end{pmatrix}; \quad (\text{D.24})$$

$$\underline{A}_{2 \times 2}^{(z)}(s) = \begin{pmatrix} 0 & -[(K_x D_1 + K_y D_3) - 1/\gamma_0^2] \\ \frac{1}{\beta_0^2} \frac{eV(s)}{E_0} h \frac{2\pi}{L} \cos \varphi & 0 \end{pmatrix} \quad (\text{D.25})$$

and  $\vec{D}$  defined by Eq. (D.6).

Here the matrix  $\underline{A}^{(1)}$  results from the synchro-betatron coupling induced by the cavities and  $\underline{A}^{(2)}$  results from the beam-beam kick.

The tune shifts induced by  $\underline{A}^{(1)}$  and  $\underline{A}^{(2)}$  can be obtained by determining the tunes with and without  $\tilde{\mathcal{H}}^1$  and  $\tilde{\mathcal{H}}^2$  or by perturbative methods as described in Ref. [18,19]. In a similar way one can calculate the distortion of the dispersion induced by the beam-beam kick.

### The Eigenvalue Spectrum of the Orbital Revolution Matrix

The solution of the original Hamiltonian (D.1) can be written as:

$$\vec{x}(s) = \underline{M}(s, s_0) \vec{x}(s_0) \quad (\text{D.26})$$

which defines the linear transfer matrix  $\underline{M}(s, s_0)$  corresponding to the variables  $(x, y, z; p_x, p_y, p_z)$ .

Note that  $\underline{M}(s, s_0)$  is symplectic [18]:

$$\underline{M}^T(s, s_0) \underline{J} \underline{M}(s, s_0) = \underline{J}. \quad (\text{D.27})$$

Thus the (normalised) eigenvectors of the revolution matrix:

$$\begin{aligned} \underline{M}(s_0 + L, s_0) \vec{v}_k(s_0) &= e^{-i2\pi Q_k} \vec{v}_k(s_0); \\ Q_{-k} &= -Q_k; \quad (k = I, II, III) \end{aligned} \quad (\text{D.28})$$

obey the orthogonality relations (see Eq. (A.4)), where we have assumed that the stability condition:

$$Q_k \text{ real number} \quad (\text{D.29})$$

is satisfied.

Putting

$$\vec{v}_k(s) = \vec{\hat{v}}_k(s) e^{-i2\pi Q_k(s/L)} \quad (\text{D.30})$$

we obtain from (D.28):

$$\vec{\hat{v}}_k(s+L) = \vec{\hat{v}}_k(s) \quad (\text{D.31})$$

(Floquet theorem). Using this result, action-angle variables for coupled motion can be introduced as described in Ref. [18].

The introduction of the dispersion has been accomplished by the matrix  $\underline{K}$  (see Eq. (D.12)):

$$\vec{\tilde{x}} = \underline{K} \vec{x}; \quad \vec{x} = \underline{K}^{-1} \vec{\tilde{x}}. \quad (\text{D.32})$$

Using the transfer matrix  $\underline{M}(s, s_0)$  we can write:

$$\vec{\tilde{x}}(s) = \underline{K}(s) \underline{M}(s, s_0) \underline{K}^{-1}(s_0) \vec{\tilde{x}}(s_0), \quad (\text{D.33})$$

showing that the transfer matrix  $\underline{\tilde{M}}(s, s_0)$  can be represented as [20]:

$$\underline{\tilde{M}}(s, s_0) = \underline{K}(s) \underline{M}(s, s_0) \underline{K}^{-1}(s_0). \quad (\text{D.34})$$

In particular one has:

$$\underline{\tilde{M}}(s_0 + L, s_0) = \underline{K}(s_0) \underline{M}(s_0 + L, s_0) \underline{K}^{-1}(s_0). \quad (\text{D.35})$$

For the eigenvectors one gets:

$$\vec{v}_k(s_0) = \underline{K}(s_0) \vec{v}_k(s_0) \quad (\text{D.36})$$

since

$$\begin{aligned} \underline{\tilde{M}}(s_0 + L, s_0) \underline{K}(s_0) \vec{v}_k(s_0) &= \underline{K}(s_0) \underline{M}(s_0 + L, s_0) \underline{K}^{-1}(s_0) \underline{K}(s_0) \vec{v}_k(s_0) \\ &= \underline{K}(s_0) \underline{M}(s_0 + L, s_0) \vec{v}_k(s_0) \\ &= e^{-i2\pi Q_k} \underline{K}(s_0) \vec{v}_k(s_0). \end{aligned} \quad (\text{D.37})$$

Note that the eigenvalues and thus the  $Q$ -values remain unchanged:

$$\tilde{Q}_k = Q_k. \quad (\text{D.38})$$

The orthogonality relations for the new eigenvectors  $\vec{v}_k$  are still valid. Furthermore,  $\underline{\tilde{M}}(s, s_0)$  is symplectic as it is obtained by a similarity transformation of  $\underline{M}$  with  $\underline{K}$ .

### Decoupled Motion; Twiss Parameters

In the case of vanishing dispersion within the cavities the revolution matrix  $\underline{\tilde{M}}(s_0 + L, s_0)$  has the simple block-diagonal form:

$$\underline{\tilde{M}}(s_0 + L, s_0) = \begin{pmatrix} \underline{M}_{(4 \times 4)}^{(\beta)}(s_0 + L, s_0) & \underline{0}_{(4 \times 2)} \\ \underline{0}_{(2 \times 4)} & \underline{M}_{(2 \times 2)}^{(z)}(s_0 + L, s_0) \end{pmatrix} \quad (\text{D.39})$$

where  $\underline{M}_{(4 \times 4)}^{(\beta)}(s_0 + L, s_0)$  corresponds to the (transverse) betatron motion and  $\underline{M}_{(2 \times 2)}^{(z)}(s_0 + L, s_0)$  to the (longitudinal) synchrotron oscillations.

Furthermore, the 2-dimensional revolution matrix  $\underline{M}_{(2 \times 2)}^{(z)}(s_0 + L, s_0)$  which is defined by the equations of synchrotron motion:

$$\begin{aligned} \frac{d}{ds} \tilde{z} &= -[(K_x \cdot D_x + K_y \cdot D_y) - 1/\gamma_0^2] \cdot \tilde{p}_z ; \\ \frac{d}{ds} \tilde{p}_z &= \frac{1}{\beta_0^2} \cdot h \cdot \frac{2\pi}{L} \cdot \frac{eV(s_0)}{E_0} \cos \varphi_0 \cdot \tilde{z} \end{aligned} \quad (\text{D.40})$$

(see Eq. (D.25)) can be represented in the form:

$$\underline{M}_{(2 \times 2)}^{(z)}(s_0 + L, s_0) = \begin{pmatrix} \cos 2\pi Q_z + \alpha_z(s_0) \cdot \sin 2\pi Q_z & \beta_z(s_0) \cdot \sin 2\pi Q_z \\ -\gamma_z(s_0) \cdot \sin 2\pi Q_z & \cos 2\pi Q_z + \alpha_z(s_0) \cdot \sin 2\pi Q_z \end{pmatrix} \quad (\text{D.41})$$

with

$$\beta_z \cdot \gamma_z = \alpha_z^2 + 1. \quad (\text{D.42})$$

From these equations one sees that the eigenvectors  $\vec{v}_k(s_0)$  can be written as:

$$\begin{aligned} \vec{v}_k &= \begin{pmatrix} \vec{v}_k^{(\beta)} \\ \vec{0}_2 \end{pmatrix}; \quad (k = I, II); \\ \vec{v}_{III} &= \begin{pmatrix} \vec{0}_4 \\ \vec{t}_z \end{pmatrix}; \quad \vec{t}_z \equiv \begin{pmatrix} t_{z1} \\ t_{z2} \end{pmatrix} = \frac{1}{\sqrt{2\beta_z(s_0)}} \cdot \begin{pmatrix} \beta_z(s_0) \\ -[\alpha_z(s_0) + i] \end{pmatrix} \cdot e^{-i\psi_z(s_0)}. \end{aligned} \quad (\text{D.43})$$

In the absence of skew quadrupoles ( $N = 0$ ) and solenoids ( $H = 0$ ) (the coupling term  $Fxy$  vanishes in (D.19)), the betatron oscillations are decoupled, leading to:

$$\underline{M}_{(4 \times 4)}^{(\beta)}(s_0 + L, s_0) = \begin{pmatrix} \underline{M}_{(2 \times 2)}^{(x)}(s_0 + L, s_0) & \underline{0}_{(2 \times 2)} \\ \underline{0}_{(2 \times 2)} & \underline{M}_{(2 \times 2)}^{(y)}(s_0 + L, s_0) \end{pmatrix};$$

$$\underline{M}_{(2 \times 2)}^{(y)}(s_0 + L, s_0) = \begin{pmatrix} \cos 2\pi Q_w + \alpha_w \sin 2\pi Q_w & \beta_w \sin 2\pi Q_w \\ -\gamma_w \sin 2\pi Q_w & \cos 2\pi Q_w + \alpha_w \sin 2\pi Q_w \end{pmatrix};$$

$$\beta_w \cdot \gamma_w = \alpha_w^2 + 1; \quad (w \equiv x, y).$$
(D.44)

As a result, the vectors  $\vec{v}_I$  and  $\vec{v}_{II}$  then take a form similar to  $\vec{v}_{III}$ :

$$\vec{v}_I^{(\beta)} = \begin{pmatrix} \vec{t}_x \\ \vec{0}_2 \end{pmatrix}; \quad \vec{v}_{II}^{(\beta)} = \begin{pmatrix} \vec{0}_2 \\ \vec{t}_y \end{pmatrix};$$

$$\vec{t}_w \equiv \begin{pmatrix} t_{w1} \\ t_{w2} \end{pmatrix} = \frac{1}{\sqrt{2\beta_w(s_0)}} \cdot \begin{pmatrix} \beta_w(s_0) \\ -[\alpha_w(s_0) + i] \end{pmatrix} \cdot e^{-i\psi_w(s_0)};$$

$$(w \equiv x, y).$$
(D.45)

It is easy to generalise this treatment to the coupled case, see Ref. [18].



## List of symbols

The symbols used in this report are listed with a brief description of the quantity they represent.

<b>Greek symbols</b>		Page
$\alpha$	crossing plane angle	3
$\alpha_i, \beta_i, \gamma_i$	Twiss parameters	38
$\beta_0$	relativistic $\beta$	30
$\gamma_0$	Lorentz factor	1
$\phi$	half crossing angle between opposite bunches	3
$\psi$	arbitrary angle parameter	17
$\tau$	artificial integration parameter	25
$\theta$	arbitrary coupling angle	1
$\theta_p$	coupling angle with respect to the principal axes	16
$\underline{\Sigma}$	beam size matrix	1
$\varphi$	substitutes $S/\cos\phi$	10
$\varphi_{RF}$	phase angle of the cavity	30
$\phi_k$	eigenphases of coupled motion	3
<b>Latin symbols</b>		Page
$\underline{A}$	transformation matrix (lab. $\Rightarrow$ acc.) for the coordinates	4
$\underline{A}^{(n)}$	transfer matrix including coupled beam-beam force and the cavity	35
$\underline{B}$	transformation matrix (lab. $\Rightarrow$ acc.) for the momenta	4
$\underline{\mathcal{B}}$	magnetic field vector	30
$\underline{C}$	transfer matrix for solenoid kick	23
$\underline{D}$	orbit dispersion function	31
$D(S)$	transformation from IP to CP	11
$D, D_{SBM}$	differential operators	21, 22
$E$	energy for test particle or bunch	4
$E_1, E_2$	horizontal, vertical principal axis of coupled motion	3
$E_h, E_v$	horizontal, vertical amplitude of the particle motion	16
$E_x, E_y$	horizontal, vertical coupling parameter	16
$\underline{T}_{bb}$	linear beam-beam matrix	29
$f$	linear beam-beam focal length	28
$F$	inverse linear beam-beam focal length including coupling	29
$F_2$	generating function	8
$F_x^*, F_y^*, F_z^*$	horizontal, vertical, longitudinal synchro-beam force	11
$g$	quadrupole strength	30
$G_x, G_y$	crossterm coupling parameters	16
$h$	harmonic number	30
$h(p_x, p_y, p_z)$	Hamiltonian in accelerator coordinates	4
$H$	solenoid field strength	19
$\mathcal{H}, \mathcal{H}_{bb}$	Hamiltonian	10
$\underline{I}$	unity matrix	24
$J_k$	invariants of coupled motion	3
$k$	mode number	2
$K_x, K_y$	horizontal, vertical curvatures	30
$\underline{K}$	transfer matrix including beam-beam and dispersion	33

Latin symbols, continued		Page
$L$	circumference of accelerator	2
$\underline{L}_0$	Lorentz boost matrix	5
$\underline{L}$	coupled Lorentz boost matrix	5
$\mathcal{L}$	Lorentz transformation	8
$\underline{M}$	6D transfer matrix	15
$N$	skew quadrupole strength	30
$N^*$	number of particles in a bunch	11
$n^*$	number of particles in a slice	11
$\mathcal{N}$	$\sqrt{[E_x^2 - E_y^2]^2 + 4(E_x G_x)^2}$	16
$\underline{0}$	zero matrix	35
$P$	momentum of the bunch	3
$p_0$	momentum of the test particle	4
$Q_{x,y,z}$	betatron tune	37
$Q_k$	betatron tune of eigenmodes	2
$\underline{R}$	crossing angle similarity transformation	5
$r_p$	classical particle radius	1
$s$	longitudinal position	4
$S$	distance between test particle and strong bunch	9
$\underline{J}$	anti-symmetric matrix of symplectic formulation	15
$\underline{T}_{bb}$	linear beam-beam matrix	29
$U$	uncoupled electric potential	1
$\hat{U}$	coupled electric potential	1
$v_k$	eigenvalues of coupled motion	3
$V$	RF voltage of the cavity	30
$\vec{x}$	coordinates of the test particle	1
$\vec{\hat{x}}$	coordinates of the coupled test particle	1
$\vec{\tilde{x}}$	coordinates of the tilted test particles	5
$\vec{x}_C$	coordinates of the transformed test particle (lab. $\Rightarrow$ acc.)	4
$\vec{x}^*$	coordinates of the Lorentz boosted test particle	6
$\vec{\tilde{x}}$	tilted coordinates of the test particle in the crossing plane	5
$\vec{\tilde{x}}^*$	coordinates of the test particle after synchro-beam mapping	5
$\vec{\tilde{x}}^*$	coordinates of the coupled test particle after synchro-beam mapping	11
$\vec{X}$	coordinates of the bunch	1
$\vec{\hat{X}}$	coordinates of the coupled bunch	3
$\vec{\tilde{X}}$	coordinates of the tilted bunch	15
$\vec{X}^\dagger$	coordinates of the slice of the bunch	8
$\hat{\vec{X}}$	coordinates of the bunch in the averaged plane	16

## Acknowledgements

We would like to thank Georges Dôme for carefully reading the manuscript. One of us (G. R.) wishes to thank the SL-AP group at CERN for making this collaboration possible by inviting him to join the group for three months. Lastly, we would like to thank Francesco Ruggiero for constant encouragement and constructive criticism.

## References

- [1] K. Hirata, H. Moshhammer and F. Ruggiero, “A Symplectic Beam-Beam Interaction with Energy Change”, KEK preprint 92-117 (1992).
- [2] K. Hirata, “Don’t Be Afraid of Beam-Beam Interactions With a Large Crossing Angle”, SLAC-PUB-6375 (1994).
- [3] H. Grote and F.C. Iselin, “The MAD program (Methodical Accelerator Design) version 8.16, User’s reference manual”, CERN/SL/90-13(AP) (rev.4) (1995).
- [4] F. Schmidt, “SixTrack, Version 1, Single particle tracking code treating transverse motion with synchrotron oscillations in a symplectic manner”, CERN/SL/90-11(AP) (1990); G. Ripken, F. Schmidt, “A Symplectic Six-Dimensional Thin-Lens Formalism for Tracking”, CERN/SL/95-12(AP) (1995), DESY 95-063 (1995);
- [5] D.P. Barber, K. Heinemann, H. Mais, G. Ripken, “A Fokker-Planck Treatment of Stochastic Particle Motion within the Framework of a Fully Coupled 6-dimensional Formalism for Electron-Positron Storage Rings including Classical Spin Motion in Linear Approximation”, DESY 91-146 (1991).
- [6] I. Borchardt, E. Karantzoulis, H. Mais, G. Ripken, “Calculation of Beam Envelopes in Storage Rings and Transport Systems in the Presence of Transverse Space Charge Effects and Coupling”, Z. Phys.C, Particles and Fields 39, (1988) p.339.
- [7] I. Borchardt, E. Karantzoulis, H. Mais, G. Ripken, “Calculation of Transverse and Longitudinal Space Charge Effects within the Framework of the Fully six-dimensional formalism”, Z. Phys.C, Particles and Fields 41, (1988) p.25.
- [8] E. Forest, K. Ohmi, “Symplectic Integration for Complex Wigglers”, KEK 92-14 (1992).
- [9] D.P. Barber, K. Heinemann, G. Ripken, F. Schmidt, “Symplectic Thin-Lens Transfer Maps for SixTrack: Treatment of Bending Magnets in Terms of the Exact Hamiltonian”, DESY 96-156 (1996).
- [10] K. Heinemann, G. Ripken and F. Schmidt, “Construction of Nonlinear Symplectic Six-Dimensional Thin-Lens Maps by Exponentiation”, DESY 95-189 (1995).
- [11] W. Gröbner, “Differentialgleichungen, Erster Teil; Gewöhnliche Differentialgleichungen”, BI-Wissenschaftsverlag (1977).
- [12] H. Mais, C. Mari, “Introduction to Beam-Beam Effects”, CERN-94-01 (1994), p.499.
- [13] G. Ripken: “Non-linear canonical equations of coupled synchro-betatron motion and their solution within the framework of a non-linear 6-dimensional (symplectic) tracking program for ultra-relativistic protons”, DESY 85-84, (1985).

- [14] D.P. Barber, G. Ripken, F. Schmidt, “A non-linear canonical formalism for the coupled synchro-betatron motion of protons with arbitrary energy”, DESY 87-36 (1987).
- [15] C.J.A. Corsten, H.J. Hagedoorn, “Simultaneous Treatment of Betatron and Synchrotron Motions in Circular Accelerators”, Nucl. Inst. Meth., vol.212, (1983) p.37.
- [16] H. Mais and G. Ripken, “Spin-Orbit Motion in a Storage Ring in the Presence of Synchrotron Radiation using a Dispersion Formalism”, DESY 86-29 (1986).
- [17] G. Ripken and E. Karantzoulis, “A Fokker-Planck Treatment of Coupled Synchro-Betatron Motion in Proton Storage Rings under the Influence of Cavity Noise”, DESY 86-29 (1986).
- [18] F. Willeke, G. Ripken, “Methods of Beam Optics”, DESY 88-114 (1988); F. Willeke, G. Ripken, “On the Impact of Linear Coupling on Nonlinear Dynamics”, DESY 90-001 (1990).
- [19] D.P. Barber, K. Heinemann, G. Ripken, F. Willeke, “Notes on Synchro-Betatron Coupling for Particles of Arbitrary Energy Using a 6-Dimensional Symplectic Dispersion Formalism”, DESY HERA 94-02 (1994).
- [20] D.P. Barber, G. Ripken, contribution to “Handbook of Accelerator Physics and Engineering”, A.W. Chao and M. Tigner, World Scientific Publishing (1999).